The Imaginary Universe (The Fine-Structure Constant is Constant, and There are Two of Them)

Szymon Łukaszyk *

Keywords: emergent dimensionality; imaginary dimensions; natural units; fine-structure constant; black holes; neutron stars; white dwarfs; patternless binary messages; complex energy; complex force; Hawking radiation; extended periodic table; general relativity; photon sphere; entropic gravity; gravitational observations; holographic principle; mathematical physics

Article

The Imaginary Universe

Szymon Łukaszyk

Łukaszyk Patent Attorneys, ul. Głowackiego 8, 40-052 Katowice, Poland; szymon@patent.pl

Abstract: Maxwell's equations in vacuum provide the negative speed of light $-c$, which leads to imaginary Planck units. However, the second, negative fine-structure constant $\alpha_2^{-1} \approx -140.178$, present in the Fresnel coefficients for the normal incidence of electromagnetic radiation on monolayer graphene, establishes the different, negative speed of light in vacuum $c_2 \approx -3.06 \times 10^8$ [m/s], which introduces imaginary Planck units different in magnitude from those parametrized with c. Furthermore, algebraic relations between the fine-structure constants hint that the fine-structure constant does not vary over time. It follows that electric charges are the same in real and imaginary dimensions. We model neutron stars and white dwarfs, emitting perfect black-body radiation, as *objects* having energy exceeding their mass-energy equivalence ratios. We define complex energies in terms of real and imaginary natural units. Their imaginary parts, inaccessible for direct observation, store the excess of these energies. It is conjectured that the maximum atomic number $Z = 238$. A black-body *object* is in the equilibrium of complex energies if its radius $R_{\text{eq}} \approx 1.3833\, R_{\text{BH}}$, which is close to the photon sphere radius $R_{\text{ps}} = 1.5\, R_{\text{BH}}$, and marginally greater than a locally negative energy density bound of $4/3\, R_{\text{BH}}$. The complex force between real masses and imaginary charges leads to the black-body object's surface gravity and the generalized Hawking radiation temperature, which includes its charge. Furthermore, this force is consistent with the Bohr model of the hydrogen atom. The proposed model takes into account the value(s) of the fine-structure constant(s), which is/are otherwise neglected in general relativity, and explains the registered (GWOSC) high masses of neutron stars' mergers and the associated fast radio bursts (CHIME) without resorting to any hypothetical types of exotic stellar *objects*.

Keywords: emergent dimensionality; imaginary dimensions; natural units; fine-structure constant; black holes; neutron stars; white dwarfs; patternless binary messages; complex energy; complex force; Hawking radiation; extended periodic table; general relativity; photon sphere; entropic gravity; gravitational observations; holographic principle; mathematical physics

---

1. Introduction

The universe began with the Big Bang, which is a current prevailing scientific opinion. But this Big Bang was not an explosion of 4-dimensional spacetime, which also is a current prevailing scientific opinion, but an explosion of dimensions. More precisely, in the -1-dimensional void, a 0-dimensional point appeared, inducing the appearance of countably infinitely other points indistinguishable from the first one. The breach made by the first operation of the *dimensional successor function* of the Peano axioms inevitably continued leading to the formation of 1-dimensional, real and imaginary lines, allowing for an ordering of points using multipliers of real units (ones) or imaginary units ($a \in \mathbb{R} \Leftrightarrow a = 1b^1$, and $a \in \mathbb{I} \Leftrightarrow a = ib$, where $b \in \mathbb{R}$). Then out of two lines of each kind, crossing each other only at one initial point $(0, 0)$, the dimensional successor function formed 2-dimensional $\mathbb{R}^2$, $\mathbb{I}^2$, and $\mathbb{R} \times \mathbb{I}$

---

[1]   This is, of course, a circular definition. But for clarity, it is given.

Euclidean planes, with $\mathbb{I}^2$ being a mirror reflection of $\mathbb{R}^2$. And so on, forming n-dimensional Euclidean spaces $\mathbb{R}^a \times \mathbb{I}^b$ with $a \in \mathbb{N}$ real and $b \in \mathbb{N}$ imaginary lines, $n := a + b$, and the scalar product defined by

$$
\mathbf{x} \cdot \mathbf{y} = (x_1, \ldots, x_a, ix'_1, \ldots, ix'_b) \, (y_1, \ldots, y_a, iy'_1, \ldots, iy'_b) :=
$$
$$
:= \sum_{k=1}^{a} x_k y_k + \sum_{l=1}^{b} x'_l \overline{y'_l}, \tag{1}
$$

where $\mathbf{x}, \mathbf{y} \in \mathbb{R}^a \times \mathbb{I}^b$. With the appearance of the first 0-dimensional point, information began to evolve [1–6].

However, the dimensional properties are not uniform. Concerning regular convex n-polytopes in natural dimensions, for example, there are countably infinitely many regular convex polygons, five regular convex polyhedra (Platonic solids), six regular convex 4-polytopes and only three regular convex n-polytopes if $n > 3$ [7]. In particular, 4-dimensional Euclidean space is endowed with a peculiar property known as exotic $\mathbb{R}^4$ [8], absent in other dimensionalities. Due to this property, $\mathbb{R}^3 \times \mathbb{I}$ space provides a continuum of homeomorphic but non-diffeomorphic differentiable structures. Each piece of individually memorized information is homeomorphic to the corresponding piece of individually perceived information but remains nondiffeomorphic (non-smooth). This allowed the variation of phenotypic traits within individuals' populations [9] and extended the evolution of information into biological evolution. Exotic $\mathbb{R}^4$ solves the problem of extra dimensions of nature, and perceived space requires a natural number of dimensions [10]. Each biological cell perceives an emergent space of three real dimensions and one imaginary (time) observer-dependently [11] and at present, when $i0 = 0$ is *real*, through a spherical Planck triangle corresponding to one bit of information in units of $-c^2$, where c is the speed of light in vacuum. This is the emergent dimensionality (ED) [5,9,12–14]. Appendix F presents some arguments to support the claim that perceived dimensionality sets favourable conditions for biological evolution to emerge.

Each dimension requires certain units of measure. In real dimensions, Max Planck in 1899 derived the *natural* units of measure as "independent of special *bodies* or *substances*, thereby necessarily retaining their meaning for all times and for all civilizations, including extraterrestrial and nonhuman ones" [15]. Planck units utilize the Planck constant h that he introduced in his black-body radiation formula. However, in 1881, George Stoney derived a system of natural units [16] based on the elementary charge e (Planck's constant was unknown then). The ratio of Stoney units to Planck units is $\sqrt{\alpha}$, where α is the fine-structure constant. This study derives the complementary set of natural units applicable to imaginary dimensions, including imaginary units, based on the discovered negative fine-structure constant α_2.

Imaginary and negative physical quantities are the subject of research. In particular, the subject of scientific research is thermodynamics in the complex plane. For example, Lee–Yang zeros [17,18] and photon-photon thermodynamic processes under negative optical temperature conditions [19] have been experimentally observed. Furthermore, the rendering of synthetic dimensions through space modulations has recently been suggested because it does not require any active materials or other external mechanisms to break the time-reversal symmetry [20]. However, physical quantities accessible for direct everyday observation are mostly real and positive with the negativity of distances, velocities, accelerations, etc., induced by the assumed orientation of *space*. Quantum measurement results, for example, are *real* eigenvalues of Hermitian operators. Unlike charges, negative, real masses are generally inaccessible for direct observation. However, dissipative coupling between excitons and photons in an optical microcavity leads to the formation of exciton polaritons with negative masses [21]. In Section 6 we show that negative masses also result from merging black-body *objects*.

Furthermore, the study introduces a model for storing the excess energy of neutron stars and white dwarfs that exceed their mass–energy equivalences in imaginary dimensions. The model results in the upper bound on the size-to-mass ratio of their cores, where the Schwarzschild radius sets the lower bound.

The paper is structured as follows. Section 2 shows that Fresnel coefficients for the normal incidence of electromagnetic radiation on monolayer graphene include the second negative fine-structure constant α_2 as a fundamental constant of nature. Section 3 shows that by this second fine-structure constant nature endows us with the α_2-natural units. Section 4 introduces the concept of a black-body *object* in thermodynamic equilibrium, emitting perfect black-body radiation, and reviews its necessary properties. Section 5 introduces complex mass and charge energies expressed in terms of real and imaginary α_2-Planck units introduced in Section 3 and applies them to black-body *objects*. Section 6 considers observed mergers of black-body *objects* to show that the observed data can be explained without the need to introduce hypothetical exotic stellar *objects*. Section 7 discusses fluctuations of black-body *objects*. Section 8 defines the complex forces that are used in Section 9 to derive a black-body *object* surface gravity and the generalized Hawking radiation temperature, and in Section 10 - in an extended Bohr model of the hydrogen atom. Section 11 summarizes the findings of this study. Certain prospects for further research are given in the Appendices.

2. The Second Fine-Structure Constant

Numerous publications provide Fresnel coefficients for the normal incidence of electromagnetic radiation (EMR) on monolayer graphene (MLG), which are remarkably defined only by π and the fine-structure constant α

$$\alpha^{-1} = \left(\frac{q_P}{e}\right)^2 = \frac{4\pi\epsilon_0 \hbar c}{e^2} \approx 137.036, \tag{2}$$

where q_P is the Planck charge, $\hbar$ is the reduced Planck constant, $\epsilon_0 \approx 8.8542 \times 10^{-12}$ [kg$^{-1}\cdot$m$^{-3}\cdot$s$^2\cdot$C^2] is vacuum permittivity (the electric constant), and e is the elementary charge. Transmittance (T) of MLG

$$T = \frac{1}{\left(1 + \frac{\pi\alpha}{2}\right)^2} \approx 0.9775, \tag{3}$$

for normal EMR incidence was derived from the Fresnel equation in the thin-film limit [22] (Equation (3)), whereas spectrally flat absorptance (A) A $\approx \pi\alpha \approx 2.3\%$ was reported [23,24] for photon energies between about 0.5 and 2.5 [eV]. T was related to reflectance (R) [25] (Equation (53)) as R $= \pi^2\alpha^2$T$/4$, i.e,

$$R = \frac{\frac{1}{4}\pi^2\alpha^2}{\left(1 + \frac{\pi\alpha}{2}\right)^2} \approx 1.2843 \times 10^{-4}, \tag{4}$$

The above equations for T and R, as well as the equation for the absorptance

$$A = \frac{\pi\alpha}{\left(1 + \frac{\pi\alpha}{2}\right)^2} \approx 0.0224, \tag{5}$$

were also derived [26] (Equations (29)–(31)) based on the thin film model (setting $n_s = 1$ for substrate). The sum of transmittance (3) and the reflectance (4) at normal EMR incidence on MLG was derived [27] (Equation (4a)) as

$$T + R = 1 - \frac{4\sigma\eta}{4 + 4\sigma\eta + \sigma^2\eta^2 + k^2\chi^2} =$$
$$= \frac{1 + \frac{1}{4}\pi^2\alpha^2}{\left(1 + \frac{\pi\alpha}{2}\right)^2} \approx 0.9776, \tag{6}$$

where $\eta \approx 376.73$ [Ω] is the vacuum impedance, $\sigma = e^2/(4\hbar) = \pi\alpha/\eta \approx 6.0853 \times 10^{-5}$ [Ω^{-1}] is the MLG conductivity [28], k is the wave vector of light in vacuum, and $\chi = 0$ is the electric susceptibility of vacuum. Therefore, these coefficients are well established theoretically and experimentally [22–24,27,29,30].

As a consequence of the conservation of energy

$$(T + A) + R = 1. \tag{7}$$

In other words, the transmittance in the Fresnel equation describing the reflection and transmission of EMR at normal incidence on a boundary between different optical media is, in the case of the 2-dimensional (boundary) of MLG, modified to include its absorption.

The reflectance R = 0.013% (4) of MLG can be expressed as the quadratic equation of α

$$R \left(1 + \frac{\pi\alpha}{2}\right)^2 - \frac{1}{4}\pi^2\alpha^2 = 0,$$
$$\frac{1}{4}(R - 1)\pi^2\alpha^2 + R\pi\alpha + R = 0, \tag{8}$$

which can be expressed in terms of the reciprocal of α, defining $\beta := 1/\alpha$ as

$$R\beta^2 + R\pi\beta + \frac{1}{4}(R - 1)\pi^2 = R\left(\beta + \frac{\pi}{2}\right)^2 - \frac{\pi^2}{4} = 0. \tag{9}$$

The quadratic Equation (9) has two roots

$$\beta = \alpha^{-1} = \frac{-\pi R + \pi\sqrt{R}}{2R} \approx 137.036, \quad \text{and} \tag{10}$$

$$\beta_2 = \alpha_2^{-1} = \frac{-\pi R - \pi\sqrt{R}}{2R} \approx -140.178. \tag{11}$$

Therefore, the Equation (8) includes the second negative fine-structure constant α_2. It turns out that the sum of the reciprocals of these fine-structure constants (10) and (11)

$$\alpha^{-1} + \alpha_2^{-1} = \frac{-\pi R + \pi\sqrt{R} - \pi R - \pi\sqrt{R}}{2R} = \frac{-2\pi}{2} = -\pi, \tag{12}$$

is remarkably independent of the value of the reflectance R. Furthermore, the minimum of the parabola (9) amounts $-\pi^2/4 \approx -2.4674$ and occurs at $-\pi/2 \approx -1.5708$, as shown in Figure 1. Also, these values are independent of the reflectance (4) value, and the same results can (only) be obtained for T + A (cf. Appendix B).
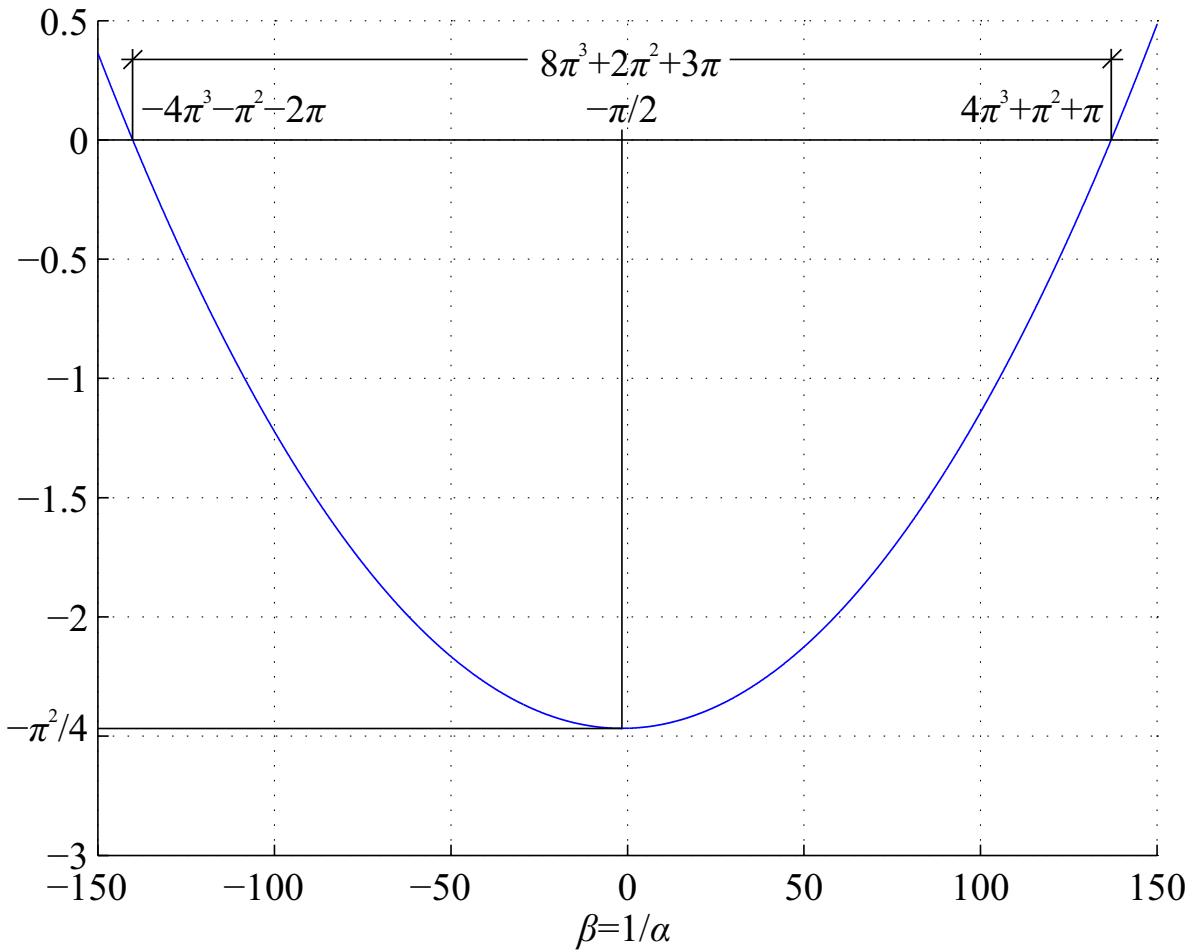
Figure 1. MLG reflectance as a function of $\beta := 1/\alpha$.

We further note that the relation (12) corresponds to the following identity

$$\frac{\alpha + \alpha_2}{\alpha \alpha_2} = -\pi, \tag{13}$$

between the roots (10) and (11), which is also present in the MLG Fresnel equations and the corresponding Euclid formula (cf. Appendix D).

These dependences on π only between the fine-structure constants α and α_2 suggest that they do not vary over time.

These results are also intriguing in the context of a peculiar algebraic expression for the fine-structure constant [31]

$$\alpha^{-1} = 4\pi^3 + \pi^2 + \pi \approx 137.036303776 \tag{14}$$

that contains a *free* π term and is very close to the physical definition (2) of α^{-1}, which according to the CODATA 2018 value is 137.035999084. We note in passing that CODATA values are computed by averaging the measurements.

Using relations (12) and (14), we can express the negative reciprocal of the 2nd fine-structure constant α_2^{-1} that emerged in the quadratic equation (8) also as a function of π only

$$\alpha_2^{-1} = -\pi - \alpha_1^{-1} = -4\pi^3 - \pi^2 - 2\pi \approx -140.177896429. \tag{15}$$

Using relations (14) and (15), T (3), R (4), and A (5) of MLG for normal incidence of EMR can be expressed just by π (cf. Appendix C). Moreover, equation (8) includes two π-like constants for two surfaces with positive and negative Gaussian curvatures (cf. Appendix E).

3. Set of α_2-Planck Units

In this section, we shall derive complementary Planck units based on the second fine-structure constant α_2. We shall further call them α_2-Planck units. Natural units can be derived from numerous starting points [5,32] (cf. Appendices G and H). The central assumption in all natural unit systems is that the quotient of the unit of length ℓ_* and time t_* is a unit of speed; we call it $c = \ell_*/t_*$. It is the speed of light in vacuum c in all systems of natural units, except for Hartree and Schrödinger units, where it is $c\alpha$, and Rydberg units, where it is $c\alpha/2^2$. On the other hand, c as the velocity of the electromagnetic wave is derivable from Maxwell's Equations in vacuum

$$\nabla^2 \mathbf{E} = \mu_0 \epsilon_0 \frac{\partial^2 \mathbf{E}}{\partial t^2}, \quad \frac{\partial^2 E}{\partial x^2} = \mu_0 \epsilon_0 \frac{\partial^2 E}{\partial t^2}, \tag{16}$$

where $\mathbf{E}$ is the electric field, and μ_0 is vacuum permeability (the magnetic constant). Without postulating any solution to this equation but by simple substitution $\partial x := \ell_*$ and $\partial t := t_*$, $\partial^2 E := E_*$ factors out, and we obtain well known

$$1 = \mu_0 \epsilon_0 c^2, \tag{17}$$

symmetric in its electric and magnetic parts [33] from which the bivalued $c = \pm 1/\sqrt{\mu_0 \epsilon_0}$ can be obtained, knowing the values of μ_0 and ϵ_0. We note that it is c^2, not c, present in mass-energy equivalence, the Lorentz factor, the BH potential, etc. We further note that Maxwell's equations in vacuum are not directly dependent on the fine-structure constant(s). It is included in the magnetic constant μ_0.

In the following, we assume the universality of the real elementary electric charge e defining both matter and antimatter, the Planck constant h, the uncertainty principle parameter, and the gravitational constant G (i.e., we assume that there are no counterparts to these physical constants in other physical dimensions in our model and that these dimensional constants are positive). The last two assumptions are probably too far-reaching, given that we do not need to know the gravitational constant G or the Planck constant h to find the product of the Planck length ℓ_P and the speed of light in vacuum [34]. We note in passing that antimatter obeys gravity [35], which is consistent with the findings of this study.

The fine-structure constant can be defined as the quotient (2) of the squared (and thus positive) elementary charge e and the squared Planck charge $\alpha = e^2/q_P^2$. We chose Planck units over other natural unit systems not only because they incorporate the fine-structure constant α and the Planck constant h. Other systems of natural units (except for Stoney units) also incorporate them. The reason is that only the Planck area defines one bit of information on a patternless black hole surface given by the Bekenstein bound (47) and the binary entropy variation [5,12].

To accommodate the negativity of the fine-structure constant discovered in the preceding section, we must introduce the imaginary Planck charge q_{Pi} so that its square would yield a negative value of α_2.

$$\begin{aligned} q_P^2 &= \frac{e^2}{\alpha} &\neq& \quad q_{Pi}^2 = \frac{e^2}{\alpha_2} \Rightarrow q_{Pi} = ae, a \in \mathbb{I}, \\ e^2 &= q_P^2 \alpha &=& \quad q_{Pi}^2 \alpha_2. \end{aligned} \tag{18}$$

Next, we note that an imaginary q_{Pi}, which must have a physical definition analogous to q_P, requires either a real and negative speed of light or some complementary real and negative electric constant (we assume that h is positive). Let us call them c_2 and $\tilde{\epsilon}_0$

$$q_P^2 = 4\pi\epsilon_0 \hbar c > 0 \quad \Leftrightarrow \quad q_{Pi}^2 = 4\pi\tilde{\epsilon}_0 \hbar c_2 < 0. \tag{19}$$

---

2   Since the square root is bivalued the unit of speed is also bivalued In Planck, Stoney, and Schrödinger units.

From this equation, we find that $\tilde{\epsilon}_0 c_2 < 0$, as the values of the other constants are known. Next, we assume that the solution (17) of Maxwell's equations in vacuum is also valid for other values of the constants involved. Let us call the unknown magnetic constant μ_2, so

$$\mu_0 \epsilon_0 c^2 = \mu_2 \tilde{\epsilon}_0 c_2^2 = 1. \tag{20}$$

From that and from $\tilde{\epsilon}_0 c_2 < 0$, we conclude that the product $\mu_2 c_2 < 0$. We note that the quotient of the squared Planck charge and mass introduces the imaginary Planck mass $m_{\mathrm{P}i}$

$$\frac{q_{\mathrm{P}}^2}{m_{\mathrm{P}}^2} = \frac{q_{\mathrm{P}i}^2}{m_{\mathrm{P}i}^2} = 4\pi\epsilon_0 G, \tag{21}$$

the value of which can be calculated, knowing the value of the imaginary Planck charge $q_{\mathrm{P}i}$ from the relation (18). From (21) we also conclude that $\tilde{\epsilon}_0 = \epsilon_0 > 0$ and then by (20) that $\mu_2 > 0$ and $c_2 < 0$. Knowing $m_{\mathrm{P}i}$ we can determine the value of the negative nonprincipal square root of $c_2 = \pm 1/\sqrt{\mu_2 \epsilon_0}$ of the relation (20) as

$$c_2 = \frac{q_{\mathrm{P}i}^2}{4\pi\epsilon_0\hbar} \approx -3.066653 \times 10^8 \ [\mathrm{m/s}], \tag{22}$$

which is greater than the speed of light in vacuum c in modulus.

The mass, length, time, and charge units can express all electrical units. Therefore, along with temperature, amount of substance, and luminous intensity, they are base units of the International System of Quantities (ISQ). We further conclude that the magnetic constant μ_2 is lower than μ_0

$$\mu_0 = \frac{4\pi\hbar\alpha}{ce^2} \approx 1.2569 \times 10^{-6} \ [\mathrm{kg} \cdot \mathrm{m} \cdot \mathrm{C}^{-2}],$$
$$\mu_2 = \frac{4\pi\hbar\alpha_2}{c_2 e^2} \approx 1.2012 \times 10^{-6} \ [\mathrm{kg} \cdot \mathrm{m} \cdot \mathrm{C}^{-2}]. \tag{23}$$

Unlike the electric constant ϵ_0, the magnetic constants μ are independent of the unit of time. Furthermore, negative α_2 and c_2 lead to the second, also time-dependent but negative vacuum impedance

$$\eta_2 = -\frac{4\pi\alpha_2\hbar}{e^2} = -\frac{1}{\epsilon_0 c_2} \approx$$
$$\approx -368.29 \ [\mathrm{kg} \cdot \mathrm{m}^2 \cdot \mathrm{s}^{-1} \cdot \mathrm{C}^{-2}] \quad (|\eta_2| < |\eta|). \tag{24}$$

Finally, combining relations (18) and (19) yields

$$e^2 = 4\pi\epsilon_0\hbar c\alpha = 4\pi\epsilon_0\hbar c_2\alpha_2, \tag{25}$$

which leads to the following important relation between the speeds of light in vacuum c, c_2, and the fine-structure constants α, α_2

$$c\alpha = c_2\alpha_2, \tag{26}$$

valid for both principal and non-principal square roots of the relation (20). $c\alpha$ is also the electron's velocity at the first circular orbit in the Bohr hydrogen atom model[3] to which we shall return in Section 10. Furthermore, the relation (26) introduces an interesting interplay between α vs. α_2 and c vs. c_2 that, as we conjecture, should be able to explain $\nu = 5/2$ state in the fractional quantum Hall effect in the 2D system of electrons, as well as other fractional states with an even

---

[3] $c\alpha$ is also the speed unit in Hartree and Schrödinger's natural units.

denominator [36] (cf. Appendix I). The relation (26) is not the only α to α_2 relation. Along with the two π-like constants π_1, π_2 (relations (A21) and (A23), cf. Appendix E)

$$\frac{\alpha_2}{\alpha} = \frac{c}{c_2} = \frac{\pi_1}{\pi} = \frac{\pi}{\pi_2} = \frac{m_P^2}{m_{Pi}^2} = \frac{q_P^2}{q_{Pi}^2} \approx -0.9776. \tag{27}$$

Therefore, the non-principal square root of $c = \pm 1/\sqrt{\mu_0 \epsilon_0}$ and principal square root of $c_2 = \pm 1/\sqrt{\mu_2 \epsilon_0}$ in (20) also introduce, respectively, imaginary $(-c)$-Planck units and real $(-c_2)$-Planck units. In particular, the imaginary $(-c)$-Planck time parameterizes the HSs time relations [5,12]. We conjecture that α_2-Planck units is appropriate for espressing physical quantities of $\mathbb{I}^3 \times \mathbb{R}$ Euclidean space rather than $\mathbb{R}^3 \times \mathbb{I}$ Euclidean space that we perceive due to the minimum energy principle (cf. Appendix F). Furthermore, the speed of electromagnetic radiation is the product of its wavelength and frequency, and these quantities would be imaginary in terms of imaginary Planck units; the negative speed of light is necessary to accommodate this.

The negative speed of light c_2 (22) leads to the complementary Planck charge q_{Pi}, length ℓ_{Pi}, mass m_{Pi}, time t_{Pi}, and temperature T_{Pi} that redefined by square roots containing c_2 raised to odd powers (1, 3, 5) become bivalued and real-imaginary since c and c_2 are bivalued. In other words, both Planck and α_2-Planck units have four forms equal in modulus: real positive, real negative, imaginary positive, and imaginary negative. However, here we consider mostly real, positive α-Planck units and imaginary, positive α_2-Planck units (hence the subscript i).

Principal square roots of the base α_2-Planck units (for negative c_2) that can be expressed, using the relation (26), in terms of base Planck units q_P, ℓ_P, m_P, t_P, and T_P are

$$q_{Pi} = \sqrt{4\pi\epsilon_0 \hbar c_n} = q_P \sqrt{\frac{\alpha}{\alpha_2}} \approx$$
$$\approx i1.8969 \times 10^{-18} \text{ [C]} \quad (|q_{Pi}| > |q_P|), \tag{28}$$

$$\ell_{Pi} = \sqrt{\frac{\hbar G}{c_n^3}} = \ell_P \sqrt{\frac{\alpha_2^3}{\alpha^3}} \approx$$
$$\approx i1.5622 \times 10^{-35} \text{ [m]} \quad (|\ell_{Pi}| < |\ell_P|), \tag{29}$$

$$m_{Pi} = \sqrt{\frac{\hbar c_n}{G}} = m_P \sqrt{\frac{\alpha}{\alpha_2}} \approx$$
$$\approx i2.2012 \times 10^{-8} \text{ [kg]} \quad (|m_{Pi}| > |m_P|), \tag{30}$$

$$t_{Pi} = \sqrt{\frac{\hbar G}{c_n^5}} = t_P \sqrt{\frac{\alpha_2^5}{\alpha^5}} \approx$$
$$\approx i5.0942 \times 10^{-44} \text{ [s]} \quad (|t_{Pi}| < |t_P|), \tag{31}$$

$$T_{Pi} = \sqrt{\frac{\hbar c_n^5}{G k_B^2}} = T_P \sqrt{\frac{\alpha^5}{\alpha_2^5}} \approx$$
$$\approx i1.4994 \times 10^{32} \text{ [K]} \quad (|T_{Pi}| > |T_P|). \tag{32}$$

Most Planck units derived from the α_2-Planck base units (28)–(32) are also imaginary. They include the α_2 Planck volume

$$\ell_{Pi}^3 = \left(\frac{\hbar G}{c_n^3}\right)^{3/2} = \ell_P^3 \sqrt{\frac{\alpha_2^9}{\alpha^9}} \approx$$
$$\approx i3.8127 \times 10^{-105} \text{ [m}^3\text{]} \quad \left(|\ell_{Pi}^3| < |\ell_P^3|\right), \tag{33}$$

the α_2 Planck momentum

$$p_{\text{P}i} = m_{\text{P}i}c_n = \sqrt{\frac{\hbar c_n^3}{G}} = m_{\text{P}}c\sqrt{\frac{\alpha^3}{\alpha_2^3}} \approx$$
$$\approx i6.7504 \ [\text{kg m/s}] \quad (|m_{\text{P}i}c_n| > |m_{\text{P}}c|) , \tag{34}$$

the α_2 Planck energy

$$E_{\text{P}i} = m_{\text{P}i}c_n^2 = \sqrt{\frac{\hbar c_n^5}{G}} = E_{\text{P}}\sqrt{\frac{\alpha^5}{\alpha_2^5}} \approx$$
$$\approx i2.0701 \times 10^9 \ [\text{J}] \quad (|E_{\text{P}i}| > |E_{\text{P}}|) , \tag{35}$$

and the α_2 Planck acceleration

$$a_{\text{P}i} = \frac{c_n}{t_{\text{P}i}} = \sqrt{\frac{c_n^7}{\hbar G}} = a_{\text{P}}\sqrt{\frac{\alpha^7}{\alpha_2^7}} \approx$$
$$\approx \pm i6.0198 \times 10^{51} \ [\text{m/s}^2] \quad (|a_{\text{P}i}| > |a_{\text{P}}|) . \tag{36}$$

However, the α_2-Planck density

$$\rho_{\text{P2}} = \frac{m_{\text{P}i}}{\ell_{\text{P}i}^3} = \frac{c_n^5}{\hbar G^2} = \rho_{\text{P}}\frac{\alpha^5}{\alpha_2^5} \approx$$
$$\approx -5.7735 \times 10^{96} \ [\text{kg/m}^3] \quad (|\rho_{\text{P2}}| > |\rho_{\text{P}}|) , \tag{37}$$

and the α_2-Planck area

$$\ell_{\text{P}i}^2 = \frac{\hbar G}{c_n^3} = \ell_{\text{P}}^2\frac{\alpha_2^3}{\alpha^3} \approx$$
$$\approx -2.4406 \times 10^{-70} \ [\text{m}^2] \quad \left(|\ell_{\text{P}i}^2| < |\ell_{\text{P}}^2|\right) , \tag{38}$$

are real and bivalued similarly to the Planck density ρ_{P} and area ℓ_{P}^2. Interestingly, both Planck forces F_{P} and

$$F_{\text{P2}} = \frac{c_2^4}{G} = \frac{c^4}{G}\frac{\alpha^4}{\alpha_2^4} = F_{\text{P}}\frac{\alpha^4}{\alpha_2^4} \approx$$
$$\approx 1.3251 \times 10^{44} \ [\text{N}] \quad (F_{\text{P2}} > F_{\text{P}}) , \tag{39}$$

are strictly positive.

We note that Coulomb's law for elementary charges and Newton's law of gravity for Planck masses define the fine-structure constants

$$\frac{1}{4\pi R_*^2}\frac{e^2}{\epsilon_0} = \alpha G\frac{m_{\text{P}}^2}{R_*^2} = \alpha_2 G\frac{m_{\text{P}i}^2}{R_*^2} , \tag{40}$$

where R_* is some real or imaginary distance and $m_{\text{P}i}$ is imaginary. The area of a disk in the denominator of the Coulomb force invites further research.

The relations between time (31) and temperature (32) α_2-Planck units are inverted, $\alpha^5 t_{Pi}^2 = \alpha_2^5 t_P^2$, $\alpha_2^5 T_{Pi}^2 = \alpha^5 T_P^2$, and saturate the energy-time version of Heisenberg's uncertainty principle (HUP) taking energy from the equipartition theorem for one bit of information [5,12,37]

$$\frac{1}{2} k_B T_P t_P = \frac{1}{2} k_B T_{Pi} t_{Pi} = \frac{\hbar}{2}. \tag{41}$$

Furthermore, eliminating α and α_2 from the relations (28)-(30), yields

$$\ell_P m_P^3 = \ell_{Pi} m_{Pi}^3 \quad \text{and} \quad \ell_P q_P^3 = \ell_{Pi} q_{Pi}^3. \tag{42}$$

Contrary to the elementary charge e (18), there is no physically meaningful *elementary mass* $M_e = \pm 1.8592 \times 10^{-9}$ [kg] that would satisfy the relation (30)

$$M_e^2 = \alpha m_P^2 = \alpha_2 m_{Pi}^2. \tag{43}$$

Neither is there a physically meaningful *elementary* (and imaginary) *length* $L_e \approx \pm i 9.7382 \times 10^{-39}$ [m] satisfying the relation (38)

$$L_e^2 = \alpha^3 \ell_{Pi}^2 = \alpha_2^3 \ell_P^2, \tag{44}$$

(which in modulus is almost 1660 times smaller than the Planck length), or an *elementary temperature* $T_e \approx \pm 6.4450 \times 10^{26}$ [K] abiding to (32)

$$T_e^2 = \alpha^5 T_P^2 = \alpha_2^5 T_{Pi}^2, \tag{45}$$

and close to the Hagedorn temperature of grand unified string models.

Planck charge relation (18) and the charge conservation principle imply that the elementary charge e is the quantum of charge in real and imaginary dimensions, while masses, lengths, temperatures, and other derived quantities that can vary with time are not similarly quantized. The universal character of the charges is additionally emphasized by the real $\sqrt{\alpha}$ multiplied by i in the imaginary charge energy (58) and imaginary $\sqrt{\alpha_2}$ in the real charge energy (59). Furthermore, the same forms of the relations (18) and (43) reflect the same forms of Coulomb's law and Newton's law of gravity, which are the inverse-square laws.

In the following, where deemed appropriate, we shall express the physical quantities by Planck units

$$\begin{aligned}
M &:= m m_P, & M_i &:= m_i m_{Pi}, & m, m_i &\in \mathbb{R} \\
E &:= m E_P & E_i &:= m_i E_{Pi}, \\
Q &:= q e, & Q_i &:= i Q = i q e, & q &\in \mathbb{Z}, \\
\lambda &:= l \ell_P, & \lambda_i &:= l_i \ell_{Pi}, & l = \tfrac{2\pi}{m}, l_i = \tfrac{2\pi}{m_i}, \\
\{R, D\} &:= \{r, d\} \ell_P, & \{R_i, D_i\} &:= \{r_i, d_i\} \ell_{Pi}, & r, d, r_i, d_i &\in \mathbb{R},
\end{aligned} \tag{46}$$

where uppercase letters M, E, Q, λ, R, and D denote respectively masses, energies, charges, Compton wavelengths, radii, and diameters (or *lengths*), lowercase letters denote multipliers of the positive real Planck units and imaginary α_2-Planck units, and the subscripts i refer to the multiplication of imaginary quantities. We note that the discretization of charges by integer multipliers q of the elementary charge e seems too far-reaching, considering the fractional charges of *quasiparticles*, in particular in the open research problem of the fractional quantum Hall effect (cf. Appendix I), and energy-dependent fractional charges in electron pairing [38].

4. Black Body Objects

There are only three observable *objects* in nature that emit perfect black-body radiation: unsupported black holes (BHs, the densest), neutron stars (NSs), supported, as accepted, by neutron

degeneracy pressure, and white dwarfs (WDs), supported, as accepted, by electron degeneracy pressure (the least dense). We shall collectively call them black-body *objects* (BBs). The spectral density in sonoluminescence, light emission by sound-induced collapsing gas bubbles in fluids, was also shown to have the same frequency dependence as black-body radiation [39,40]. Thus, the sonoluminescence, and in particular *shrimpoluminescence* [41], is probably emitted by collapsing micro-BBs. Micro-BH induced in glycerin by modulating acoustic waves was reported [42].

The term "black-body object" is not used in general relativity (GR) and standard cosmology, but standard cosmology scrunches under embarrassingly significant failings, not just *tensions* as is sometimes described, as if to somehow imply that a resolution will eventually be found [43]. Also, James Webb Space Telescope data show multiple galaxies that grew too massive too soon after the Big Bang, which is a strong discrepancy with the Λ cold dark matter model (ΛCDM) expectations on how galaxies formed at early times at both redshifts, even when considering observational uncertainties [44]. This is an important unresolved issue indicating that fundamental changes to the reigning ΛCDM model of cosmology are needed [44]. The term *object* as a collection of *matter* is a misnomer as it neglects the (quantum) nonlocality [45] that is independent of the entanglement among *particles* [46], as well as the Kochen-Specker contextuality [47], and increases as the number of *particles* grows [48,49]. Thus, we use emphasis for (perceivably indistinguishable) *particle* and (perceivably distinguishable) *object*, as well as for *matter* and *distance*. The ugly duckling theorem [50,51] asserts that every two *objects* we perceive are equally similar (or equally dissimilar), however ridiculous and contrary to common sense[4] that may sound. These terms do not have an absolute meaning in ED. In particular, given the observation of *quasiparticles* in classical systems [52]. Within the framework of ED no *object* is *enclosed* in *space*.

Entropic gravity [37] explains the galaxy rotation curves without resorting to dark matter (which is not required to explain the rotation curves of certain galaxies, such as the massive relic galaxy NGC 1277 [53]), has been experimentally confirmed [54], and is decoherence-free [55]. It has been experimentally confirmed that the so-called *accretion instability* is a fundamental physical process [56]. We conjecture that this process, already recreated under laboratory conditions [57], is common for all BBs. As black-body radiation is radiation of global thermodynamic equilibrium, it is patternless [58] (thermal noise) radiation that depends only on one parameter. In the case of BHs, this is known as Hawking [59] radiation, and this parameter is the BH temperature $T_{BH} = T_P/(2\pi d_{BH})$ corresponding to the BH diameter [5] $D_{BH} = d_{BH}\ell_P$, where $d_{BH} \in \mathbb{R}$. Furthermore, BHs absorb patternless information [5,60]. Therefore, since Hawking radiation depends only on the diameter of a BH, it is the same for a given BH, even though it is momentary as the BH fluctuates (cf. Section 7).

As black-body radiation is patternless, triangulated [5] BBs contain a balanced number of Planck area triangles, each having binary potential $\delta\varphi_k = -c^2 \cdot \{0, 1\}$, as has been shown for BHs [5], based on the Bekenstein-Hawking (BH) entropy [61] $S_{BH} = k_B N_{BH}/4$, where $N_{BH} := 4\pi R_{BH}^2/\ell_P^2 = \pi d_{BH}^2$ is the information capacity of the BH surface, i.e., the $\lfloor N_{BH} \rfloor \in \mathbb{N}_0$ Planck triangles[5] corresponding to bits of information [5,12,37,61,62], and the fractional part triangle(s) having the area $\{N_{BH}\}\ell_P^2 = (N_{BH} - \lfloor N_{BH} \rfloor)\ell_P^2$ too small to carry a single bit of information [5,12].

BH entropy can be derived from the Bekenstein bound

$$S \leq \frac{2\pi k_B R E}{\hbar c} = \pi k_B m d, \tag{47}$$

which defines an upper limit on the thermodynamic entropy S that can be contained within a sphere of radius R and energy E. Substituting BH (Schwarzschild) radius $R_{BH} = 2GM_{BH}/c^2$ and mass-energy

---

[4]   Which inevitably enforces understanding the nature in a manner that is *common* to nearly all people and thus hinders its research.

[5]   "$\lfloor x \rfloor$" is the floor function that yields the greatest integer less than or equal to its argument x.

equivalence $E_{\mathrm{BH}} = M_{\mathrm{BH}}c^2$, where M_{BH} is the BH mass, into the bound (47), it reduces to the BH entropy. In other words, the BH entropy saturates the Bekenstein bound (47)[6].

The patternless nature of perfect black-body radiation was derived [5] by comparing the BH entropy with the binary entropy variation $\delta S = k_{\mathrm{B}}N_1/2$ ([5] Eq. (55)), valid for any holographic sphere (HS), where $N_1 \in \mathbb{N}$ denotes the number of active Planck triangles with binary potential $\delta\varphi_k = -c^2$. Thus, the entropy of all BBs is

$$S_{\mathrm{BB}} = \frac{1}{4}k_{\mathrm{B}}N_{\mathrm{BB}}. \tag{48}$$

Furthermore, $N_1 = N_{\mathrm{BB}}/2$ confirms the patternless thermodynamic equilibrium of BBs by maximizing Shannon entropy [5].

We shall define the generalized radius of a BB (this definition applies to all HSs) having mass M_{BB} as a function of GM_{BB}/c^2 multiplier $k \in \mathbb{R}, k \geq 2$

$$R_{\mathrm{BB}} := k\frac{GM_{\mathrm{BB}}}{c^2}, \quad d_{\mathrm{BB}} = 2km_{\mathrm{BB}}, \tag{49}$$

and the generalized BB energy E_{BB} as a function of $M_{\mathrm{BB}}c^2$ multiplier $a \in \mathbb{R}$ (this definition also applies to all HSs)

$$E_{\mathrm{BB}} := aM_{\mathrm{BB}}c^2, \quad E_{\mathrm{BB}} = am_{\mathrm{BB}}E_{\mathrm{P}}. \tag{50}$$

Substituting M_{BB} from definition (49) into definition (50) and the latter into the Bekenstein bound (47), it becomes

$$S \leq \frac{1}{2}k_{\mathrm{B}}\frac{a}{k}N_{\mathrm{BB}}, \tag{51}$$

and equals the BB entropy (48) if $\frac{a}{2k} = \frac{1}{4} \Rightarrow a = \frac{k}{2}$. Thus, the energy of all BBs having a generalized radius (49) is

$$E_{\mathrm{BB}} = \frac{k}{2}M_{\mathrm{BB}}c^2 = \frac{k}{2}m_{\mathrm{BB}}E_{\mathrm{P}} = \frac{d_{\mathrm{BB}}}{4}E_{\mathrm{P}}, \tag{52}$$

with $k = 2$ in the case of BHs, setting the lower bound for other BBs. We shall further call the coefficient k the *size-to-mass ratio* (STM). It is similar to the specific volume (the reciprocal of density) of the BB. We shall derive the upper STM bound in Section 5.

According to the no-hair theorem, all BHs general relativity (GR) solutions are characterized only by three parameters: mass, electric charge, and angular momentum. However, BHs are fundamentally uncharged, since the parameters of any conceivable BH, in particular, charged (Reissner–Nordström) and charged-rotating (Kerr–Newman) BH, can be arbitrarily altered, provided that the BH area does not decrease [63] using Penrose processes [64,65] to extract electrostatic and/or rotational energy of BH [66]. Thus any BH is defined by only one real parameter: its diameter, mass, temperature, energy, etc., each corresponding to the other. We note that in the complex Euclidean $\mathbb{R}^a \times \mathbb{I}^b$ space, an n-ball ($n = a + bi \in \mathbb{C}$) is spherical only for a vanishing imaginary dimension and for the radius $r = 1/\sqrt{\pi}$ ($R = \ell_{\mathrm{P}}/\sqrt{\pi}$) [12,14], resulting in its information capacity $N = 4$, one unit of BH entropy [61]. This confirms the universality and applicability of the BH entropy (48) to all BBs.

Interiors of the BBs are inaccessible to an exterior observer [61], which makes them similar to interior-less mathematical points representing real numbers on a number line[7]. Yet, a BH can embrace this defining real number. Three points forming a Planck triangle corresponding to a bit of information on a BH surface can store this parameter, and this is intuitively comprehensible: the area of a spherical triangle is larger than that of a flat triangle defined by the same vertices, provided the curvature is nonvanishing and depends on this curvature, i.e., this additional parameter defines it. Thus, the only

---

[6] Furthermore, the Bekenstein bound can be derived from the BH entropy: $S_{\mathrm{BH}} = k_{\mathrm{B}}\pi RR/\ell_{\mathrm{P}}^2 \leq k_{\mathrm{B}}\pi R\frac{2GE}{c^4}\frac{c^3}{\hbar G}$, where we used $M \leq \frac{Rc^2}{2G}$ and $E = Mc^2$.

[7] Thus, the term *object* is a particularly staring misnomer if applied to BBs.

meaningful *spatial* notion is the Planck area triangle, which encodes one bit of classical information and its curvature.

However, it is accepted that in the case of NSs, electrons combine with protons to form neutrons, so that NSs are composed almost entirely of neutrons. But it is never the case that all electrons and all protons of an NS become neutrons. WDs are charged by definition, as they are accepted to be mostly composed of electron degenerate *matter*. But how can a charged BB store both the curvature and an additional parameter corresponding to its charge? Fortunately, the relation (18) ensures that the charges are the same in real and imaginary dimensions. Therefore, each *charged* Planck triangle of a BB surface is associated with at least three $\mathbb{R} \times \mathbb{I}$ Planck triangles, each sharing a vertex or two vertices with this triangle in $\mathbb{R}^2$. And this configuration is capable of storing both the curvature and the charge. The Planck area ℓ_P^2 (38) and the $\mathbb{R} \times \mathbb{I}$ imaginary Planck area $\ell_P \ell_{Pi} = \ell_P^2 \sqrt{\alpha_2^3/\alpha^3} \approx \pm 0.9666 i \ell_P^2$, which is smaller in modulus, can be considered in a polyspherical coordinate system, in which gravitation/acceleration acts in a radial direction (with the entropic gravitation acting inwardly and acceleration acting in both radial directions) [5], while electrostatics act in a tangential direction.

Contrary to the no-hair theorem, we characterize BBs only by mass and charge, neglecting the angular momentum since the latter introduces the notion of time, which we find redundant in the BB description of a patternless thermodynamical equilibrium.

Not only BBs are perfectly spherical. Also, their mergers, to which we shall return in Section 6, are perfectly spherical, as it has been experimentally confirmed [67] based on the registered gravitational event GW170817. One can hardly expect a collision of two perfectly spherical, patternless thermal noises to produce some aspherical pattern instead of another perfectly spherical patternless noise. Where would the information about this pattern come from at the moment of the collision? From the point of impact? No point of impact is distinct on a patternless surface.

The considerations previously discussed may be confusing to the reader, as the energy (52) of BBs other than BHs (i.e., for $k > 2$) exceeds the mass-energy equivalence $E = Mc^2$, which is the limit of the maximum *real* energy. In the following section, we will model a part of the energy of NS and WD that exceeds Mc^2 as imaginary and thus unmeasurable.

5. BB Complex Energies

A complex energy formula

$$E_R := E_{M_R} + iE_{Q_R} = M_R c^2 + \frac{iQ_R}{2\sqrt{\pi\epsilon_0 G}} c^2, \tag{53}$$

where E_{M_R} and iE_{Q_R} represent respectively real and imaginary energy of an *object* having mass M_R and charge Q_R[8] was proposed in ref. [68]. Equation (53) considers real masses M_R and charges Q_R. To store the surplus energy we shall modify it to a form involving real physical quantities expressed terms in Planck units and imaginary physical quantities expressed terms of the imaginary α_2-Planck units using relations (25), (26), (30), (35) and (46)

$$\frac{e}{2\sqrt{\pi\epsilon_0}} = \sqrt{\alpha c \hbar} = \sqrt{\alpha_2 c_2 \hbar}. \tag{54}$$

---

[8]   Charges in the cited study are defined in CGS units. Here, we adopt SI.

To this end, we define the following three complex energies, linking the mass, imaginary mass, and charge within the ED framework, the complex energy of real mass and imaginary charge

$$E_{MQ_i} := E_M + E_{Q_i} = Mc^2 + \frac{Q_i}{2\sqrt{\pi\epsilon_0 G}}c^2 =$$
$$= \left(mm_{\mathrm{P}} + iq\sqrt{\alpha}m_{\mathrm{P}}\right)c^2 = \left(m + iq\sqrt{\alpha}\right)E_{\mathrm{P}}, \tag{55}$$

of real charge and imaginary mass

$$E_{QM_i} := E_Q + E_{M_i} = \frac{Q}{2\sqrt{\pi\epsilon_0 G}}c_2^2 + M_i c_2^2 =$$
$$= \left(q\sqrt{\alpha_2}m_{\mathrm{P}i} + m_i m_{\mathrm{P}i}\right)c_2^2 = \frac{\alpha^2}{\alpha_2^2}\left(q\sqrt{\alpha} + \sqrt{\frac{\alpha}{\alpha_2}}m_i\right)E_{\mathrm{P}}, \tag{56}$$

and of real mass and imaginary mass

$$E_{MM_i} := Mc^2 + M_i c_2^2 = \left(m + \sqrt{\frac{\alpha^5}{\alpha_2^5}}m_i\right)E_{\mathrm{P}}, \tag{57}$$

as illustrated in Figure 2.
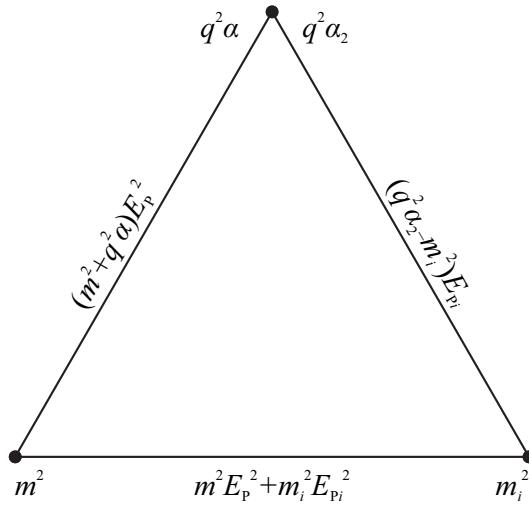
Figure 2. Illustration of three complex energies linking mass m, imaginary mass m_i, and charge q.

We neglect the energy of real and imaginary charges E_{QQ_i}, since by the relation (18), the unit of charge is the same in real and imaginary dimensions. The mass-energy equivalence relates the mass M or M_i to the speed of light c or c_2.

Energies (55) and (56) yield two different charge energies corresponding to the elementary charge, the imaginary quantum

$$E_{Q_i}(q = \pm 1) = \pm i\sqrt{\alpha}E_{\mathrm{P}} \approx \pm i 1.6710 \times 10^8 \text{ [J]}, \tag{58}$$

and the - larger in modulus - real quantum

$$E_Q(q = \pm 1) = \pm\sqrt{\alpha_2}E_{\mathrm{P}i} \approx \pm 1.7684 \times 10^8 \text{ [J]}. \tag{59}$$

Furthermore, $\forall q, \alpha^2 E_{Qi} = i\alpha_2^2 E_Q$.

The squared moduli of the complex energies (55)-(57), expressed in terms of the Planck energy, are

$$|E_{MQ_i}|^2 = \left(M^2 + q^2 \alpha m_{\mathrm{P}}^2 \right) c^4 = \left(m^2 + q^2 \alpha \right) E_{\mathrm{P}}^2, \tag{60}$$

$$|E_{QM_i}|^2 = \frac{\alpha^4}{\alpha_2^4} \left(q^2 \alpha m_{\mathrm{P}}^2 - M_i^2 \right) c^4 = \frac{\alpha^4}{\alpha_2^4} \left(q^2 \alpha - \frac{\alpha}{\alpha_2} m_i^2 \right) E_{\mathrm{P}}^2, \tag{61}$$

$$|E_{MM_i}|^2 = \left(M^2 - \frac{\alpha^4}{\alpha_2^4} M_i^2 \right) c^4 = \left(m^2 - \frac{\alpha^5}{\alpha_2^5} m_i^2 \right) E_{\mathrm{P}}^2. \tag{62}$$

Theorem 1. *Complex energies* (55)–(57) *cannot simultaneously have their real and imaginary parts equal in modulus.*

Proof. Complex energies E_{MQ_i} and E_{QM_i} are real-to-imaginary *balanced* if their real and imaginary parts are equal in modulus. This holds for

$$q^2 \alpha = m^2 = -\frac{\alpha}{\alpha_2} m_i^2. \tag{63}$$

However, they cannot be simultaneously balanced with the energy E_{MM_i}, which is balanced for

$$m^2 = -\frac{\alpha^5}{\alpha_2^5} m_i^2 \neq -\frac{\alpha}{\alpha_2} m_i^2. \tag{64}$$

□

Since by the relation (18) charges are the same in real and imaginary dimensions, squared moduli of complex energies E_{MQ_i} and E_{QM_i} must be equal, allowing us to obtain the value of the imaginary mass M_i as a function of mass M and charge Q in this equilibrium

$$m_i = \pm \sqrt{ \frac{\alpha_2}{\alpha} \left[q^2 \alpha \left(1 - \frac{\alpha_2^4}{\alpha^4} \right) - \frac{\alpha_2^4}{\alpha^4} m^2 \right] }. \tag{65}$$

In particular for $q = 0$ the relation (65) yields

$$m_i^2 = -\frac{\alpha_2^5}{\alpha^5} m^2 \quad \text{or} \quad M_i = \pm i \frac{\alpha_2^2}{\alpha^2} M \approx \pm 0.9557 i M, \tag{66}$$

which corresponds to the relation (64). Since the mass $m_i \in \mathbb{R}$, the square root argument must be nonnegative in relation (65)

$$m \geq |q| \sqrt{ \alpha \left(\frac{\alpha^4}{\alpha_2^4} - 1 \right) } \approx |q| 0.0263. \tag{67}$$

This means that the masses of uncharged micro-BHs ($q = 0$) in thermodynamic equilibrium can be arbitrary. However, micro NSs and micro WDs, also in thermodynamic equilibrium, are charged. Thus, even a single elementary charge ($q = 1$) of a white dwarf renders its mass $M_{\mathrm{WD}} = 5.7275 \times 10^{-10}$ [kg] comparable to the mass of a grain of sand.

We note here that only the masses satisfying $M < 2\pi m_{\mathrm{P}} \approx 1.3675 \times 10^{-7}$ [kg] have Compton wavelengths larger than Planck length [5]. We note in passing that a classical description has been

ruled out on the microgram (1×10^{-9} [kg]) mass scale [69]. Comparing this bound with the bound (67) yields the charge multiplier q corresponding to an atomic number

$$
Z = \left\lfloor \left| \frac{2\pi}{\sqrt{\alpha\left(\frac{\alpha^4}{\alpha_2^4} - 1\right)}} \right| \right\rfloor = \lfloor 238.7580 \rfloor = 238, \tag{68}
$$

of a hypothetical element, which - as we conjecture - sets the limit on an extended periodic table and is a little higher than the accepted limit of $Z = 184$ (unoctquadium). More massive elements would have Compton wavelengths smaller than the Planck length, which is physically implausible because the Planck area is the smallest area required to encode one bit of information [5,37,61,62]. From the relation (67) we can also obtain the maximum wavelength $l = 2\pi/m$ corresponding to the charge q. For $q^2 = 1$ it is $\lambda < 3.8589 \times 10^{-33}$ [m] with $l < 238.7580$ corresponding to the bound (68).

Theorem 2. *Complex energies* (55)–(57) *are equal*

$$
|E_{MQ_i}|^2 = |E_{QM_i}|^2 = |E_{MM_i}|^2 =
$$
$$
= \left(1 + \frac{\alpha_2^4}{\alpha^4}\right) m^2 E_P^2 = \left(1 + \frac{\alpha_2^4}{\alpha^4}\right) q^2 \alpha E_P^2 = \left(1 + \frac{\alpha_2^4}{\alpha^4}\right) \frac{\alpha^9}{\alpha_2^9} m_i^2 E_P^2 \tag{69}
$$

for

$$
q^2 \alpha = -\frac{\alpha^5}{\alpha_2^5} m_i^2 = \frac{\alpha_2^4}{\alpha^4} m^2, \quad m_i^2 = -\frac{\alpha_2^9}{\alpha^9} m^2. \tag{70}
$$

Proof. Direct calculation proves the relation (70) and if the squared moduli (60)–(62) are equal to some constant energy

$$
|E_{MQ_i}|^2 = |E_{QM_i}|^2 = |E_{MM_i}|^2 := A^2 E_P^2, \tag{71}
$$

then subtracting $|E_{MQ_i}|^2 - |E_{QM_i}|^2$ yields

$$
m^2 + \frac{\alpha}{\alpha_2} m_i^2 = A^2 \left(1 - \frac{\alpha_2^4}{\alpha^4}\right); \tag{72}
$$

subtracting this from $|E_{MM_i}|^2$ yields

$$
m_i^2 = -A^2 \frac{\alpha_2^9}{\alpha^5(\alpha^4 + \alpha_2^4)}, \tag{73}
$$

which substituted into the relation (72) yields

$$
m^2 = A^2 \frac{\alpha^4}{\alpha^4 + \alpha_2^4}, \tag{74}
$$

and finally, substituting the relation (74) into the modulus (60) yields

$$
q^2 \alpha = A^2 \frac{\alpha_2^4}{\alpha^4 + \alpha_2^4}. \tag{75}
$$

$\square$

We can interpret the squared generalized energy of BBs (52) as the squared modulus of the complex energy of the real mass E_{MQ_i}, taking the observable real energy $E_{BB} = M_{BB}c^2$ of the BB as the real part of this energy. Thus

$$\frac{k^4}{4}m_{BB}^2 = m_{BB}^2 + q_{BB}^2\alpha, \quad q_{BB}^2\alpha = m_{BB}^2\left(\frac{k^2}{4} - 1\right), \tag{76}$$

where $q_{BB}^2\alpha$ represents a charge surplus energy exceeding $M_{BB}c^2$. Similarly, we can interpret the squared generalized energy of BBs (52) as the squared modulus of the complex energy of the imaginary mass E_{QM_i}. Thus

$$\frac{k^2}{4}m_{BB}^2 = \frac{\alpha^4}{\alpha_2^4}\left(q_{BB}^2\alpha - \frac{\alpha}{\alpha_2}m_{iBB}^2\right). \tag{77}$$

Substituting $q_{BB}^2\alpha$ from the relation (76) into the relation (77) turns the equilibrium condition (65) into a function of the STM k instead of the charge q

$$m_{iBB} = \pm m_{BB}\sqrt{\frac{\alpha_2}{\alpha}\left[\frac{k^2}{4}\left(1 - \frac{\alpha_2^4}{\alpha^4}\right) - 1\right]}, \tag{78}$$

which yields the imaginary mass of a BH (for $k = 2$) and corresponds to the relation (66) between uncharged masses M and M_i, which is, notably, independent of the STM. The square root argument in the relation (78) must be non-negative, since $m_{BB}, m_{iBB} \in \mathbb{R}$. This leads to the maximum STM bound

$$k \leq \frac{2}{\sqrt{1 - \frac{\alpha_2^4}{\alpha^4}}} \approx 6.7933 = k_{max}. \tag{79}$$

The relations (76) and (78) are shown in Figure 3.
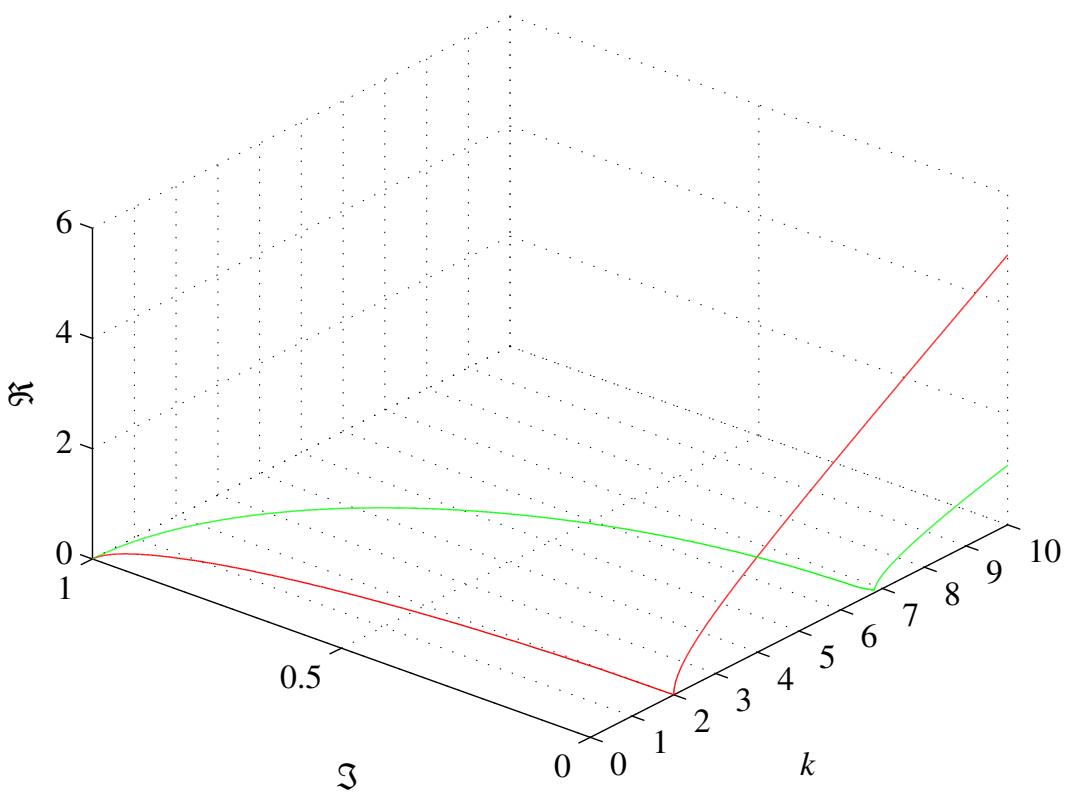
Figure 3. Ratios of imaginary mass $M_{i\text{BB}}$ to real mass M_{BB} (green) and real charge $q_{\text{BB}} m_{\text{P}} \sqrt{\alpha}$ to M_{BB} (red) of a BB as a function of the size-to-mass ratio $0 \le k \le 10$. The mass $M_{i\text{BB}}$ is imaginary for $k \lessapprox 6.79$. The charge q_{BB} is real for $k \ge 2$.

Furthermore, using the relation (26), from (78) we obtain the relation between real and imaginary BH energies $E_{\text{BH}i} = \pm i E_{\text{BH}}$, which are equal in modulus. In general, the relation (78) relates BBO energies as

$$E_{\text{BBI}i}^2 = E_{\text{BB}}^2 \left[\frac{\alpha^4}{\alpha_2^4} \left(\frac{k^2}{4} - 1 \right) - \frac{k^2}{4} \right]. \tag{80}$$

The maximum STM bound $k_{\max}$ (79) sets the bounds on the BB energy (52), mass, and radius (49)

$$R_{\text{BH}} = \frac{2GM_{\text{BB}}}{c^2} \le R_{\text{BB}} \le \frac{k_{\max} G M_{\text{BB}}}{c^2}. \tag{81}$$

In particular, using the relations (46), $2m_{\text{BB}} \le r_{\text{BB}} \le k_{\max} m_{\text{BB}}$ or $r_{\text{BB}}/k_{\max} \le m_{\text{BB}} \le r_{\text{BB}}/2$.

Furthermore, the relations (67) and (79) expresed in terms of the generalized radius (49) $k = d_{\text{BB}}/(2m_{\text{BB}})$ set the bound on the BB minimum mass if $|E_{MQ_i}|^2 = |E_{QM_i}|^2$

$$m_{\text{BB}} > \max \left\{ q_{\text{BB}} \sqrt{\alpha \left(\frac{\alpha^4}{\alpha_2^4} - 1 \right)}, \frac{d_{\text{BB}}}{4} \sqrt{1 - \frac{\alpha_2^4}{\alpha^4}} \right\}, \tag{82}$$

where

$$q_{\text{BB}}^2 \alpha = \frac{d_{\text{BB}}^2}{16} \frac{\alpha_2^4}{\alpha^4} \tag{83}$$

defines a condition in which neither q_{BB} nor d_{BB} can be further increased to reach its counterpart (defined, respectively, by d_{BB} and q_{BB}) in the bound (82). Thus, for example, 1-bit BB ($d_{\text{BB}} = 1/\sqrt{\pi}$)

corresponds to $q_{\text{BB}} > 1.5780$, π-bit BB ($d_{\text{BB}} = 1$) corresponds to $q_{\text{BB}} > 2.7969$, while the conjectured heaviest element with atomic number q_{BB} (68) corresponds to

$$d_{\text{BB}} = \pm \frac{8\pi}{\sqrt{1 - \frac{\alpha_2^4}{\alpha^4}}} \approx \pm 85.3666. \tag{84}$$

In the case of a BB, we obtain the equality of all three complex energies (55)-(57) substituting $A = m_{\text{BB}} k / 2$ from (49) into the relation (71) and comparing this with (69). This yields

$$k_{\text{eq}} = 2 \sqrt{1 + \frac{\alpha_2^4}{\alpha^4}} \approx 2.7665, \tag{85}$$

at which all three energies are equal. The equilibrium k_{eq} (85) and the maximum k_{max} (79) STMa satisfy $k_{\text{eq}}^2 + 16/k_{\text{max}}^2 = 8$.

The BB in the energy equilibrium k_{eq} bearing the elementary charge ($q^2 = 1$) would have mass $M_{\text{BB}_{\text{eq}}} \approx \pm 1.9455 \times 10^{-9}$ [kg], imaginary mass $M_{i\text{BB}_{\text{eq}}} \approx \pm i 1.7768 \times 10^{-9}$ [kg], wavelength $\lambda_{\text{BB}_{\text{eq}}} \approx \pm 1.1361 \times 10^{-33}$ [m], and imaginary wavelength $\lambda_{i\text{BB}_{\text{eq}}} \approx \pm i 1.2160 \times 10^{-33}$ [m]. On the other hand, the relation (76) provides the charge of the BB in equilibrium (71) as $q_{\text{BB}}(k_{\text{eq}}) \approx 11.1874 \, m_{\text{BB}}$ and the limit of the BB charge $q_{\text{BB}}(k_{\text{max}}) \approx 37.9995 \, m_{\text{BB}}$

We note that BBs with STMs $2 \leq k \leq 3$ are referred to in state of the art as *ultracompact* [70], where $k = 3$ is a photon sphere radius[9]. Any *object* that undergoes complete gravitational collapse passes through an ultracompact stage [71], where $k < 3$. Collapse can be approached by gradual accretion, increasing the mass to the maximum stable value, or by loss of angular momentum [71]. During the loss of angular momentum, the star passes through a sequence of increasingly compact configurations until it finally collapses to become a black hole. It was also pointed out [72] that for a neutron star of constant density, the pressure at the center would become infinite if $k = 2.25$, a radius of the maximal sustainable density for gravitating spherical *matter* given by Buchdahl's theorem. It was shown [73] that this limit applies to any well-behaved spherical star where density increases monotonically with radius. Furthermore, some observers would measure a locally negative energy density if $k < 2.6(6)$ thus breaking the dominant energy condition, although this may be allowed [74]. As the surface gravity grows, photons from further behind the NS become visible. At $k \approx 3.52$ the whole NS surface becomes visible [75]. The relative increase in brightness between the maximum and minimum of a light curve are greater in the case of $k < 3$ than in the case of $k > 3$ [75]. Therefore the equilibrium STM ratio $k_{\text{eq}} \approx 2.7665$ (85) is well within the range of radii of ultracompact *objects* researched in state-of-the-art within the framework of GR.

However, aside from the Schwarzschild radius, derivable from escape velocity $v_{esc}^2 = 2GM/R$ of mass M by setting $v_{esc}^2 = c^2$, and discovered in 1783 by John Michell [76], all the remaining significant radii of GR are only approximations[10]. GR neglects the value of the fine-structure constants α and α_2, which, similarly to π or the base of the natural logarithm, are the fundamental constants of nature.

---

9   At which, according to an accepted photon sphere definition, the strength of gravity *forces photons to travel in orbits*. The author wonders why the photons would not *travel in orbits* at a radius $R = GM/c^2$ corresponding to the *orbital* velocity $v_{\text{orb}}^2 = GM/R$ of mass M. Obviously, photons do not *travel*.

10 One may find constructive criticism of GR in [77–83].

6. BB Mergers

As the entropy (Boltzmann, Gibbs, Shannon, von Neumann) of independent systems is additive, a merger of BB_1 and BB_2 having entropies[11] (48) $S_1 = \frac{1}{4} k_B N_1$ and $S_2 = \frac{1}{4} k_B \pi d_2^2$, produces a BB_C having entropy

$$S_1 + S_2 = S_C \quad \Leftrightarrow \quad d_1^2 + d_2^2 = d_C^2, \tag{86}$$

which shows that the resultant information capacity is the sum of the information capacities of the merging components. Thus, a merger of two primordial BHs, each having the Planck length diameter, the reduced Planck temperature $\frac{T_P}{2\pi}$ (the largest physically significant temperature [12]), and no tangential acceleration a_{LL} [5,12], produces a BH having $d_{BH} = \pm\sqrt{2}$ which represents the minimum BH diameter allowing for the notion of time [12]. In comparison, a collision of the latter two BHs produces a BH having $d_{BH} = \pm 2$ having the triangulation defining only one precise diameter between its poles (cf. [5] Figure 3(b)), which is also recovered from HUP (cf. Appendix G).

Substituting the generalized diameter (49) into the entropy relation (86) establishes a Pythagorean relation between the generalized energies (52) of the merging components and the merger

$$\frac{k_C^2}{4} m_C^2 = \frac{k_1^2}{4} m_1^2 + \frac{k_2^2}{4} m_2^2, \quad \forall m_k \in \{\mathbb{R}, \mathbb{I}\}. \tag{87}$$

It is accepted that gravitational events' observations alone allow measuring the masses of the merging components, setting a lower limit on their compactness, but it does not exclude mergers more compact than neutron stars, such as *quark stars*, BHs, or more exotic *objects* [84]. We note in passing that describing the registered gravitational events as *waves* is misleading - normal modulation of the gravitational potential, registered by LIGO and Virgo interferometers, and caused by rotating (in the merger case, inspiral) *objects*, is wrongly interpreted as a gravitational wave understood as a carrier of gravity [85]. Furthermore, it has been hinted that outside GR, merging BHs may differ from their GR counterparts [86].

The accepted value of the Chandrasekhar WD mass limit, which prevents its collapse into a denser form, is $M_{Ch} \approx 1.4 \, M_\odot$ [87] and the accepted value of the analogous Tolman–Oppenheimer–Volkoff NS mass limit is $M_{TOV} \approx 2.9 \, M_\odot$ [88,89]. There is no accepted value of the BH mass limit. The conjectured value is $5 \times 10^{10} \, M_\odot \approx 9.95 \times 10^{40}$ kg. We note in passing that a BH with a surface gravity equal to the Earth's surface gravity (9.81 m/s²) would require a diameter of $D_{BH} \approx 9.16 \times 10^{15}$ m (slightly less than one light year) [5] and mass $M_{BH} \approx 3.08 \times 10^{42}$ kg exceeding the conjectured limit. The masses of most registered merging components go well beyond M_{TOV}. Of those that do not, most of the total or final masses exceed this limit. Therefore, these mergers are classified as BH mergers. Only a few are classified otherwise, including GW170817, GW190425, GW200105, and GW200115, listed in Table 1.

Table 1. Selected BB mergers discovered with LIGO and Virgo. Masses in $M_\odot$.

Event	M_1	M_2	M_C	k_1	k_2	k_C
GW170817	$1.46^{+0.12}_{-0.10}$	$1.27^{+0.09}_{-0.09}$	2.8	4.39	4.39	3.03
GW190425	$2.00^{+0.6}_{-0.2}$	$1.4^{+0.3}_{-0.3}$	$3.4^{+0.3}_{-0.1}$	4.39	4.39	3.15
GW200105	$8.9^{+1.2}_{-1.5}$	$1.9^{+0.3}_{-0.2}$	$10.9^{+1.1}_{-1.2}$	2.76	4.39	2.38
GW200115	$5.7^{+1.8}_{-2.1}$	$1.5^{+0.7}_{-0.3}$	$7.1^{+1.5}_{-1.4}$	3	4.39	2.64

The relation (87) explains the measurements of large masses of the BB mergers with at least one charged merging component without resorting to any hypothetical types of exotic stellar *objects* such as *quark stars*. Interferometric data, available online at the Gravitational Wave Open Science Center

---

[11] We drop the HS subscripts in this section for clarity.

(GWOSC) portal[12], indicates that the total mass of a merger is the sum of the masses of the merging components. Thus

$$
\begin{aligned}
m_C &= m_1 + m_2, \\
m_C^2 &= m_1^2 + m_2^2 + 2m_1m_2, \\
m_C^2 &\begin{cases} \geq m_1^2 + m_2^2 & \text{if} \quad m_1m_2 \geq 0 \\ \leq m_1^2 + m_2^2 & \text{if} \quad m_1m_2 \leq 0 \end{cases}.
\end{aligned}
\tag{88}
$$

We can use the squared moduli $|E_{MQ_i}|^2$, $|E_{QM_i}|^2$, and $|E_{MM_i}|^2$ to derive some information about the merger from the relation (87). We shall initially assume $m_k \geq 0 \Rightarrow m_1m_2 \geq 0$, since negative masses, similar to negative lengths, and their products with positive ones, are (in general [21]) inaccessible for direct observation, unlike charges. $|E_{MQ_i}|^2$ with the first inequality (88) yields

$$
\begin{aligned}
|E_{MQ_i}|_C^2 &= |E_{MQ_i}|_1^2 + |E_{MQ_i}|_2^2, \\
m_C^2 &= m_1^2 + m_2^2 + (q_1^2 + q_2^2)\alpha - q_C^2\alpha \geq m_1^2 + m_2^2, \\
q_C^2 &\leq q_1^2 + q_2^2,
\end{aligned}
\tag{89}
$$

On the other hand, $|E_{QM_i}|^2$ with the inequality (89) lead to ($\alpha_2 < 0$), so the direction of the inequality is reversed)

$$
q_C^2 \leq q_1^2 + q_2^2 \quad \Rightarrow \quad m_{iC}^2 \geq m_{i1}^2 + m_{i2}^2.
\tag{90}
$$

But $|E_{MM_i}|^2$ with the first inequality (88) lead to

$$
m_C^2 \geq m_1^2 + m_2^2 \quad \Rightarrow \quad m_{iC}^2 \leq m_{i1}^2 + m_{i2}^2,
\tag{91}
$$

contradicting the inequality (90) ($\alpha_2^5 < 0$), while $|E_{MM_i}|^2$ with the inequality (90) lead to

$$
m_{iC}^2 \geq m_{i1}^2 + m_{i2}^2 \quad \Rightarrow \quad m_C^2 \leq m_1^2 + m_2^2,
\tag{92}
$$

contradicting the first inequality (88) and consistent with the second inequality (88) introducing the product of positive and negative masses. $|E_{QM_i}|^2$ with the inequality (91) yields

$$
m_{iC}^2 \leq m_{i1}^2 + m_{i2}^2 \quad \Rightarrow \quad q_C^2 \geq q_1^2 + q_2^2,
\tag{93}
$$

contradicting the inequality (90) and so on.

The additivity of the entropy (86) of statistically independent merging BBs, both in global thermodynamic equilibrium, defined by their generalized radii (49), introduces the energy relation (87). This relation, equality of charges in real and imaginary dimensions (18), and the BB complex energies (60)–(62) induce imaginary, negative, and mixed masses during the merger. Thus, the BB merger spreads in all dimensions, not only observable ones, as a gravitational event associated with a fast radio burst (FRB) event, as reported [90] based on the gravitational event GW1904251 and the FRB 20190425A event[13]. Furthermore, IXPE[14] observations show that the detected polarized X-rays from 4U 0142+61 pulsar exhibit a 90° linear polarization swing from low to high photon energies [91]. In addition, direct evidence for a magnetic field strength reversal based on the observed sign change and extreme variation of FRB 20190520B's rotation measure, which changed from ~ 10000 [rad $\cdot$ m^{-2}]

---

[12]   https://www.gw-openscience.org/eventapi/html/allevents
[13]   Data available online at the Canadian Hydrogen Intensity Mapping Experiment (CHIME) portal (https://www.chime-frb.ca/catalog).
[14]   X-ray Polarimetry Explorer (https://ixpe.msfc.nasa.gov).

to $\sim -16000\ [\text{rad} \cdot \text{m}^{-2}]$ between June 2021 and January 2022 has been reported [92]; such extreme rotation measure reversal has never been observed before in any FRB or any astronomical object.

In the observable dimensions during the merger, the STM ratio k_C decreases, making the BB_C denser until it becomes a BH for $k_C = 2$ and no further charge reduction is possible (cf. Fig 3). From the relation (87) and the first inequality (88) we see that this holds for

$$k_C^2 \left(M_1^2 + M_2^2 \right) \le k_1^2 M_1^2 + k_2^2 M_2^2. \tag{94}$$

For two merging BHs $k_1 = k_2 = 2$ and the relation (94) yields $k_C^2 \le 4 \Rightarrow k_C = 2 = k_{\text{BH}_C}$.

Table 1 lists the mass-to-size ratios k_{BB_C} calculated according to the relation (87) that provide the measured mass M_{BB_C} of the merger and satisfy the inequality (94). The mass-to-size ratios k_{BB_1} and k_{BB_2} of the merging components were arbitrarily selected on the basis of their masses, taking into account the limit of mass M_{TOV} of the NS.

7. BB Fluctuations

A relation [93] (p.160) describing a BH information capacity, having an initial information capacity[15] $N_j = 4\pi R_j^2 / \ell_P^2$, after absorption of a *particle* having the Compton wavelength equal to the BH radius R_j

$$N_{j+1}^A = 64\pi^3 \frac{\ell_P^2}{R_j^2} + 32\pi^2 + 4\pi \frac{R_j^2}{\ell_P^2}, \tag{95}$$

was subsequently generalized [5] (Equation (18)) to all Compton wavelengths $\lambda = l\ell_P = \frac{2\pi}{m} \ell_P$ (or frequencies $\nu = c/\lambda = 1/(lt_P)$) and thus to all radiated Compton energies $E = mE_P, m \in \mathbb{R}$ absorbed $(+)$ or emitted $(-)$ by a BH as

$$N_{j+1}^{A/E}(m) = 16\pi m^2 \pm 8\pi dm + \pi d^2. \tag{96}$$

The relation (96) can be further generalized, using the generalized diameter $d = 2k\hat{m}$ (49), to all BBs as

$$\Delta N^{A/E} := N_{j+1}^{A/E}(k, m) - N_j = 16\pi m \left(m \pm k\hat{m} \right), \tag{97}$$

where $\hat{m}$ represents the BB mass, and its roots are

$$m^{A/E} = \{0, \mp k\hat{m}\} = \left\{ 0, \mp \frac{d}{2} \right\} = \{0, \mp r\}, \tag{98}$$

where it vanishes.

---

[15]   We drop the HS subscripts in this section for clarity.
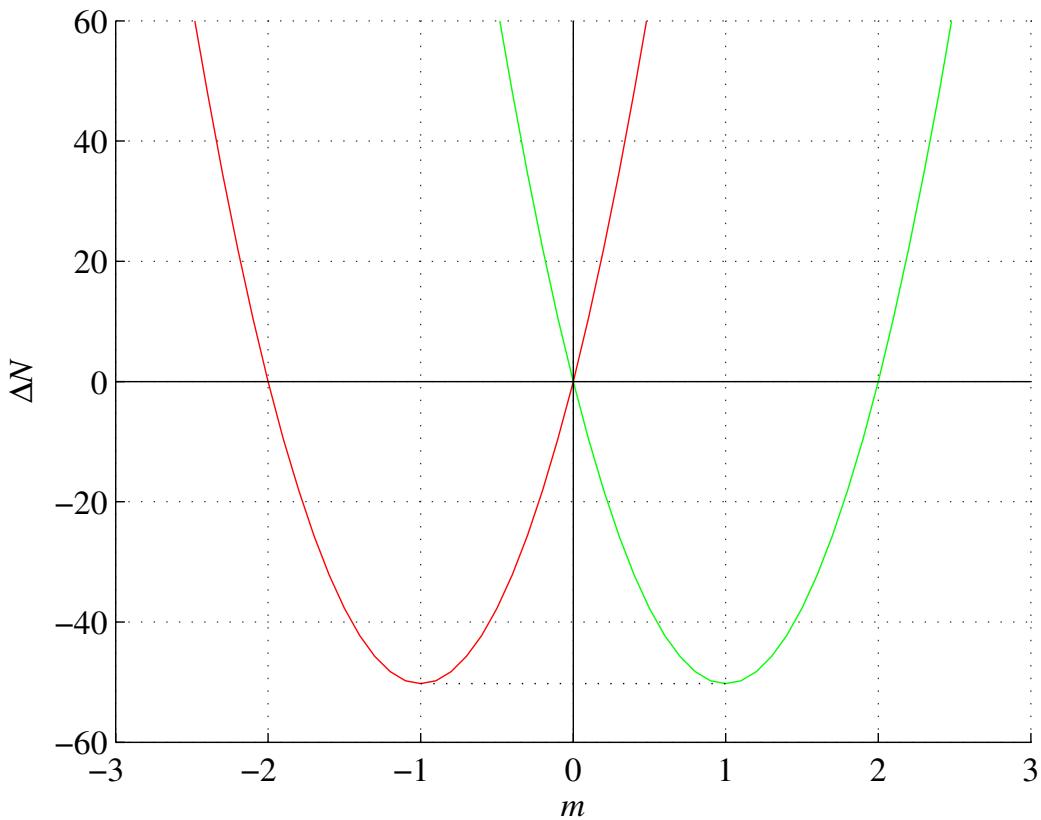
Figure 4. BB information capacity variations ΔN after absorption (red) or emission (green) of energy m ($k = 2$, $\hat{m} = 1$).

Thus, in general, a BB changes its information capacity by

$$
\Delta N^A \begin{cases} > 0 & m \in (-\infty, -k\hat{m}) \cap (0, \infty) \\ = 0 & m = \{-k\hat{m}, 0\} \\ < 0 & m \in (-k\hat{m}, 0) \end{cases},
$$

$$
\Delta N^E \begin{cases} > 0 & m \in (-\infty, 0) \cap (k\hat{m}, \infty) \\ = 0 & m = \{0, k\hat{m}\} \\ < 0 & m \in (0, k\hat{m}) \end{cases}, \tag{99}
$$

absorbing or emitting energy m with $\min(\Delta N) = -4\pi k^2 \hat{m}^2$ at $m = \pm k\hat{m}/2$, as shown in Figure 4. The relation (99) shows that, depending on its mass $\hat{m}$, a BB can expand or contract by emitting or absorbing energy m [5]. However, expansion by emission ($\Delta N^E > 0$), for example, requires energy $m > k\hat{m}$ exceeding the mass-energy equivalence of BB for $k > 2$, which is consistent with the results presented in Section 5.

8. Complex Forces

Coulomb's force F_C between two charges is positive or negative, depending on the sign and type (real or imaginary) of the charges, as summarized below in the case of some real distance separating the charges

$$
\begin{array}{c|c|c}
 & q_1q_2 > 0 & q1q_2 < 0 \\
\hline
Q_k = q_ke & F_C > 0 & F_C < 0 \\
Q_k = iq_ke & F_C < 0 & F_C > 0
\end{array}
\tag{100}
$$

Newton's law of universal gravitation is also positive or negative, depending on the sign and type of masses, as summarized below

$$
\begin{array}{c|c|c}
 & m_{*1}m_{*2} > 0 & m_{*1}m_{*2} < 0 \\
\hline
M_k = m_km_P & F_G > 0 & F_G < 0 \\
M_{ik} = m_{ik}m_{Pi} & F_{2G} < 0 & F_{2G} > 0
\end{array}
\tag{101}
$$

In the case of an imaginary distance, the signs of the inequalities are opposite. We do not consider *mixed* real or imaginary radii and mixed forces (based on real and imaginary masses/charges) as the real and imaginary dimensions are orthogonal.

Complex energies (55)–(57) define complex forces (similarly to the complex energy of real masses and charges (53), [68] Equation (7)) acting over real and imaginary *distances* R, R_i. Using the relations (46), we obtain the following products

$$
\begin{aligned}
E_{1mq_i}E_{2mq_i} &:= E_{1MQ_i}E_{2MQ_i}/E_P^2 = \\
&= m_1m_2 - q_1q_2\alpha + i\sqrt{\alpha}(m_1q_2 + m_2q_1),
\end{aligned}
\tag{102}
$$

$$
\begin{aligned}
E_{1qm_i}E_{2qm_i} &:= E_{1QM_i}E_{2QM_i}/E_P^2 = \\
&= \frac{\alpha^4}{\alpha_2^4}\left(\alpha q_1q_2 + \frac{\alpha}{\alpha_2}m_{i1}m_{i2} + \sqrt{\frac{\alpha}{\alpha_2}}\sqrt{\alpha}\,(q_1m_{i2} + q_2m_{i1})\right),
\end{aligned}
\tag{103}
$$

$$
\begin{aligned}
E_{1mm_i}E_{2mm_i} &:= E_{1MM_i}E_{2MM_i}/E_P^2 \\
&= m_1m_2 + \frac{\alpha}{\alpha_2}m_{i1}m_{i2} + \sqrt{\frac{\alpha^5}{\alpha_2^5}}\,(m_1m_{i2} + m_2m_{i1}),
\end{aligned}
\tag{104}
$$

defining three complex forces acting over a real *distance R*

$$
F_{AB_i} = \frac{G}{c^4R^2}E_{1AB_i}E_{2AB_i} = \frac{F_P}{r^2}E_{1ab_i}E_{2ab_i},
\tag{105}
$$

and three complex forces acting over an imaginary *distance R_i*

$$
\tilde{F}_{AB_i} = \frac{G}{c_2^4R_i^2}E_{1AB_i}E_{2AB_i} = \frac{\alpha_2}{\alpha}\frac{F_P}{r_i^2}E_{1ab_i}E_{2ab_i},
\tag{106}
$$

where $A, B \in \{M, Q\}$ and $a, b \in \{m, q\}$, and

$$
\alpha_2 r^2 F_{AB_i} = \alpha r_i^2 \tilde{F}_{AB_i}.
\tag{107}
$$

With a further simplifying assumption of $r^2 = r_i^2$, the forces acting on a real *distance R* are stronger and opposite to the corresponding forces acting on an imaginary *distance R_i* even though the Planck force is lower than the α_2-Planck force (39). This is a strong assumption, but seemingly correct. The general radius (49) and energy (52) are the same in Planck units and in α_2-Planck units; STM remains the same.

9. BB Complex Gravity and Temperature

We can use the complex force F_{MQ_i} (105) with the product (102) (i.e., complex Newton's law of universal gravitation) to calculate the BB surface gravity g_{BB}, assuming an uncharged ($q_2 = 0$) test mass m_2 and comparing this force with Newton's 2nd law of motion

$$\frac{F_P}{r_{BB}^2} \left(m_{BB}m_2 + i\sqrt{\alpha}m_2 q_{BB} \right) =$$
$$= M_2 g_{BB} = m_2 m_P \hat{g}_{BB} a_P,$$
$$\hat{g}_{BB} = \frac{1}{r_{BB}^2} \left(m_{BB} + i\sqrt{\alpha}q_{BB} \right), \tag{108}$$

where $g_{BB} = \hat{g}_{BB} a_P, \hat{g}_{BB} \in \mathbb{R}$. Substituting $q_{BB}\sqrt{\alpha}$ from the BB equilibrium relation (76) and mass taken from the generalized BB radius (49) $r_{BB} = km_{BB}$ into the relation (108) yields

$$\hat{g}_{BB} = \frac{1}{kr_{BB}} \left(1 \pm i\sqrt{\frac{k^2}{4} - 1} \right), \tag{109}$$

which reduces to BH surface gravity for $k = 2$ and in modulus

$$\hat{g}_{BB}^2 = \frac{1}{k^2 r_{BB}^2} \left(1 + i\sqrt{\frac{k^2}{4} - 1} \right) \left(1 - i\sqrt{\frac{k^2}{4} - 1} \right) = \frac{1}{4r_{BB}^2}. \tag{110}$$

for all k. In particular,

$$g_{BB}(k_{max}) = \pm\frac{a_P}{d_{BB}} \left(0.2944 \pm 0.9557i \right), \tag{111}$$

$$g_{BB}(k_{eq}) = \pm\frac{a_P}{d_{BB}} \left(0.7229 \pm 0.6909i \right). \tag{112}$$

The BB surface gravity (109) leads to the generalized complex Hawking blackbody-radiation equation

$$T_{BB} = \frac{\hbar}{2\pi c k_B} g_{BB} = \frac{T_P}{k\pi d_{BB}} \left(1 \pm i\sqrt{\frac{k^2}{4} - 1} \right), \tag{113}$$

describing the BB temperature[16] by including its charge in the imaginary part, which also for $k = 2$ and in modulus reduces to BH temperature for all k.

In particular,

$$T_{BB}(k_{max}) = \pm\frac{T_P}{2\pi d_{BB}} \left(\frac{\sqrt{\alpha^4 - \alpha_2^4}}{\alpha^2} \pm i\frac{\alpha_2^2}{\alpha^2} \right),$$
$$= \pm\frac{T_P}{2\pi^3 d_{BB}} \left(\sqrt{\pi^4 - \pi_1^4} \pm i\pi_1^2 \right),$$
$$= \pm\frac{T_P}{2\pi\pi_2^2 d_{BB}} \left(\sqrt{\pi_2^4 - \pi^4} \pm i\pi^2 \right), \tag{114}$$

---

16   In a commonly used form it is $T_{BB} = \frac{\hbar c^3}{2k^2\pi G M_{BB} k_B} \left(1 \pm i\sqrt{\frac{k^2}{4} - 1} \right)$.

$$T_{\mathrm{BB}}(k_{\mathrm{eq}}) = \pm \frac{T_{\mathrm{P}}}{2\pi d_{\mathrm{BB}}} \frac{\alpha^2 \pm i\alpha_2^2}{\sqrt{\alpha^4 + \alpha_2^4}},$$

$$= \pm \frac{T_{\mathrm{P}}}{2\pi d_{\mathrm{BB}}} \frac{\pi^2 \pm i\pi_1^2}{\sqrt{\pi^4 + \pi_1^4}} = \pm \frac{T_{\mathrm{P}}}{2\pi d_{\mathrm{BB}}} \frac{\pi_2^2 \pm i\pi^2}{\sqrt{\pi_2^4 + \pi^4}},$$

(115)

reduce to the BH temperature for $\alpha_2 = 0$. We note that for $d_{\mathrm{BB}} = 1$, $\mathrm{Re}(T_{\mathrm{BB}}(k_{\max})) \approx 6.6387 \times 10^{30}$ [K] has the magnitude of the Hagedorn temperature of strings, while $T_{\mathrm{P}}/(2\pi) \approx 2.2549 \times 10^{31}$ [K]. It seems, therefore, that a universe without α_2-imaginary dimensions (i.e., with $\alpha_2 = 0$) would be a black hole. Hence, the evolution of information [1–6] requires imaginary time. And we cannot zero α_2 as we would have to neglect the *existence* of graphene.

10. Hydrogen Atom

The Bohr model of the hydrogen atom is based on three assumptions that can be conveniently expressed in terms of Planck units, using the relations (46). The assumption of a natural number of electron wavelengths λ_e that fits along the circumference of the electron's orbit of radius R becomes

$$n\lambda_e = 2\pi R \quad \Leftrightarrow \quad nl_e = 2\pi r, \quad n \in \mathbb{N}.$$

(116)

De Broglie's relation between electron mass M_e, velocity V_e and wavelength becomes

$$\lambda_e = \frac{h}{M_e V_e} = \frac{2\pi\hbar}{M_e V_e} \quad \Leftrightarrow \quad l_e = \frac{2\pi}{m_e v_e}, \; V_e = v_e c, v_e \in \mathbb{R}.$$

(117)

Finally, the postulated equality between the centripetal force exerted on the electron *orbiting around* the proton (assuming an infinite mass of the latter) and the Coulomb force between the electron and the proton[17] becomes

$$\frac{M_e V_e^2}{R} = \frac{1}{4\pi\epsilon_0} \frac{e^2}{R^2} \quad \Leftrightarrow \quad m_e v_e^2 r = \frac{e^2}{4\pi\epsilon_0 \hbar c} = \alpha.$$

(118)

It is remarkable that such a simple postulate expressed in terms of Planck units introduces the fine-structure constant α. Joining the relations (116) and (117) yields

$$m_e v_e r = n,$$

(119)

which combined with (118) and using the relation (26) yields

$$V_e = v_e c = \frac{1}{n}\alpha c = \frac{1}{n}\alpha_2 c_n \quad \Leftrightarrow \quad v_e = \frac{1}{n}\alpha,$$

(120)

Thus, at the first circular orbit ($n = 1$) in this model $v_e = \alpha$.

---

[17] In the Bohr model of atoms other than hydrogen this equality of forces is *extended* to a point-like set of Z electrons orbiting around a nucleus, where Z is the atomic number. Furthermore, since the proton and the electron have different signs of the elementary charge e, the Coulomb force should be considered negative in this model.

We shall now assume that the centripetal force acting on the electron is equal to the complex force F_{MQ_i} (105) with the product of real mass and imaginary charge energies (102) and use the reduced mass of the proton-electron system

$$\frac{m_e m_p}{m_e + m_p} \frac{v_e^2}{r} = \frac{m_e m_p + \alpha + i\sqrt{\alpha}(m_e - m_p)}{r^2},$$

$$v_e^2 = \frac{m_e + m_p}{r}\left(1 + \frac{\alpha}{m_e m_p}\right) + i\frac{\sqrt{\alpha}}{r}\frac{m_e^2 - m_p^2}{m_e m_p}, \qquad (121)$$

$$r = \frac{m_e + m_p}{v_e^2}\left(1 + \frac{\alpha}{m_e m_p}\right) + i\frac{\sqrt{\alpha}}{v_e^2}\frac{m_e^2 - m_p^2}{m_e m_p},$$

where $q_e = -1$ and $q_p = 1$ are the electron and proton charges, and $M_p = m_p m_{\mathrm{P}}$, $m_p \in \mathbb{R}$ is the proton mass.

For the electron mass $M_e = 9.1094 \times 10^{-31}$ [kg] and the proton mass $M_p = 1.6726 \times 10^{-27}$ [kg] the equation (121) yields $v_e \approx 7.2993 \times 10^{-3} - i3.2816 \times 10^{-21} \approx \alpha$ assuming that R is equal to the Bohr radius $a_0 = 5.2918 \times 10^{-11}$ [m] or the radius $R \approx (5.2946 \times 10^{-11} - i4.7607 \times 10^{-29})$ [m] $\approx a_0$ assuming that the Bohr model gives the velocity of the electron, that is, $v_e = \alpha$.

We note that these values correspond to the values given by the Bohr model. We further note that neglecting the opposite signs of the charges ($q_e = q_p = -1$ or $q_e = q_p = 1$) in the relation (121) yields, respectively, an imaginary electron velocity $v_e \approx 3.2852 \times 10^{-21} \pm i7.2993 \times 10^{-3} \approx \pm i\alpha$ and a negative radius $R \approx (-5.2947 \times 10^{-11} \pm i4.7660 \times 10^{-29})$ [m] $\approx -a_0$. We further note that switching the signs of charges ($q_e = 1$, $q_p = -1$) provides complex conjugates of the relation (121), which in this case describes the antihydrogen. Therefore, we conjecture that the energy generated during a hydrogen-antihydrogen collision is

$$E_{H-\bar{H}} = 2(m_e m_p + \alpha)E_{\mathrm{P}} \approx 2.8549 \times 10^7 [\mathrm{J}]. \qquad (122)$$

Finally, we note that the relation (121) based, as the Bohr model, on the mass of the electron provides a better agreement to the Bohr radius and the fine-structure constant since

$$m_e v_e^2 r = m_e m_p + \alpha + i\sqrt{\alpha}(m_e - m_p),$$

$$r = \frac{m_p}{\alpha^2} + \frac{1}{m_e \alpha} + i\alpha^{-3/2}\left(1 - \frac{m_p}{m_e}\right) \approx \frac{1}{m_e \alpha} = \frac{a_0}{\ell_{\mathrm{P}}}, \qquad (123)$$

$$v_e^2 = \alpha m_e m_p + \alpha^2 + i\alpha^{3/2}(m_e - m_p) \approx \alpha^2.$$

11. Discussion

The reflectance of graphene under the normal incidence of electromagnetic radiation expressed as the quadratic equation for the fine-structure constant α includes the 2nd negative fine-structure constant α_2. The sum of the reciprocal of this 2nd fine-structure constant α_2 with the reciprocal of the fine-structure constant α (2) is independent of the reflectance value R and is remarkably equal to simply $-\pi$. The particular algebraic definition of the fine-structure constant $\alpha^{-1} = 4\pi^3 + \pi^2 + \pi$, containing the free π term, can be interpreted as the asymptote of the CODATA value α^{-1}, the value of which varies with time. The negative fine-structure constant α_2 leads to the α_2-Planck units applicable to imaginary dimensions, including imaginary α_2-Planck units (28)–(36). Furthermore, the elementary charge e is common for real and imaginary dimensions (18).

Applying α_2 Planck units to a complex energy formula [68] yields complex energies (55), (56) setting the atomic number $Z = 238$ as the limit on an extended periodic table. The generalized energy (52) of all perfect black-body *objects* (black holes, neutron stars and white dwarfs) having the generalized radius $R_{\mathrm{BB}} = kR_{\mathrm{BH}}/2$ exceeds the mass-energy equivalence if $k > 2$. The complex energies (55)–(57) allow storing the excess of this energy in their imaginary parts. The results show that

the perfect black-body *objects* other than black holes cannot have masses lower than 5.7275×10^{-10} [kg] and that $k_{\max} \approx 6.7933\,k \leq 6.7933$ defined by the relation (79). In addition, it is shown that a black-body *object* is in the equilibrium of complex energies if its radius $R_{\mathrm{eq}} \approx 1.3833\,R_{\mathrm{BH}}$ (85). The proposed model explains the registered (GWOSC) high masses of the neutron star mergers without resorting to any hypothetical types of exotic stellar *objects*.

In the context of the results of this study, monolayer graphene, a truly 2-dimensional material with no thickness[18], is a *keyhole* to other, unperceivable dimensionalities. The history of graphene is also instructive. Discovered in 1947 [95], graphene was long considered an *academic material* until it was eventually pulled from graphite in 2004 [96] by means of ordinary Scotch tape[19]. These fifty-seven years, along with twenty-nine years (1935-1964) between the condemnation of quantum theory as *incomplete* [97] and Bell's mathematical theorem [98] asserting that it is not true, and the fifty-eight years (1964-2022) between the formulation of this theorem and 2022 Nobel Prize in Physics for its experimental *loophole-free* confirmation, should remind us that Max Planck, the genius who discovered Planck units, has also discovered Planck's principle.

Acknowledgments: I truly thank my wife Magdalena Bartocha for her support ever since this research [99,100] began. I thank Wawrzyniec Bieniawski for inspiring discussions and constructive ideas concerning the layout of this paper and his feedback while working on the BB mergers and BB fluctuations sections. I thank Andrzej Tomski for the definition of the scalar product for Euclidean spaces $\mathbb{R}^a \times \mathbb{I}^b$ (1).

Appendix A Abbreviations

The following abbreviations are used in this paper:

ED   emergent dimensionality
EMR   electromagnetic radiation
MLG   monolayer graphene
T   transmittance
R   reflectance
A   absorptance
HUP   Heisenberg's uncertainty principle
DOF   degree of freedom
BH   black hole
NS   neutron star
WD   white dwarf
BB   black-body object
HS   holographic sphere
STM   size-to-mass ratio
GR   general relativity

Appendix B Other MLG Quadratic Equations

The quadratic equation for the sum of transmittance (3) and absorptance (5) of MLG under normal incidence of EMR corresponds to Equation (8), substituting $R = 1 - T - A$. However, the sums of the roots of other quadratic equations are not independent on T, A, or R. For example, the sum of T + R (6) expressed as the quadratic equation (substituting $C_{\mathrm{TR}} := T + R$) is

$$\frac{1}{4}\left(C_{\mathrm{TR}} - 1\right)\pi^2\alpha^2 + C_{\mathrm{TR}}\pi\alpha + \left(C_{\mathrm{TR}} - 1\right) = 0, \tag{A1}$$

---

[18]   Thickness of MLG is reported [94] as 0.37 [nm] with other reported values up to 1.7 [nm]. However, considering that 0.335 [nm] is the established inter-layer *distance* and consequently the thickness of bilayer graphene, these results do not seem credible: the thickness of bilayer graphene is not $2 \times 0.37 + 0.335 = 1.075$ [nm].

[19]   Introduced into the market in 1932.

and has two roots with reciprocals

$$\alpha^{-1} = \frac{\pi(C_{TR} - 1)}{-2C_{TR} + 2\sqrt{2C_{TR} - 1}} \approx 137.036, \tag{A2}$$

and

$$\alpha_{TR}^{-1} = \frac{\pi(C_{TR} - 1)}{-2C_{TR} - 2\sqrt{2C_{TR} - 1}} \approx 0.0180, \tag{A3}$$

whereas their sum

$$\alpha_{TR_1}^{-1} + \alpha_{TR_2}^{-1} = \frac{-\pi C_{TR}}{C_{TR} - 1} \approx 137.054 \tag{A4}$$

is dependent on T and R, which hints that in the case of MLG, transmittance (3) and absorptance (5) should be considered together as their sum.

Appendix C Mlg Transmittance, Absorptance, and Reflectance as Functions of π Only

With algebraic definitions of α (14) and α_2 (15), T (3), R (4) and A (5) of MLG for normal EMR incidence can be expressed just by π. For $\alpha^{-1} = 4\pi^3 + \pi^2 + \pi$ (14) they become

$$T(\alpha) = \frac{4(4\pi^2 + \pi + 1)^2}{(8\pi^2 + 2\pi + 3)^2} \approx 0.9775, \tag{A5}$$

$$A(\alpha) = \frac{4(4\pi^2 + \pi + 1)}{(8\pi^2 + 2\pi + 3)^2} \approx 0.0224, \tag{A6}$$

while for $\alpha_2^{-1} = -4\pi^3 - \pi^2 - 2\pi$ (15) they become

$$T(\alpha_2) = \frac{4(4\pi^2 + \pi + 2)^2}{(8\pi^2 + 2\pi + 3)^2} \approx 1.0228, \tag{A7}$$

$$A(\alpha_2) = -\frac{4(4\pi^2 + \pi + 2)}{(8\pi^2 + 2\pi + 3)^2} \approx -0.0229, \tag{A8}$$

with

$$R(\alpha) = R(\alpha_2) = \frac{1}{(8\pi^2 + 2\pi + 3)^2} \approx 1.2843 \times 10^{-4}. \tag{A9}$$

$(T(\alpha) + A(\alpha)) + R(\alpha) = (T(\alpha_2) + A(\alpha_2)) + R(\alpha_2) = 1$ as required by the law of energy conservation (7), whereas each conservation law is associated with a certain symmetry, as asserted by Noether's Theorem. $A(\alpha) > 0$ and $A(\alpha_2) < 0$ imply a *sink* and a *source* respectively, while the opposite holds for T, as illustrated schematically in Figure A1.
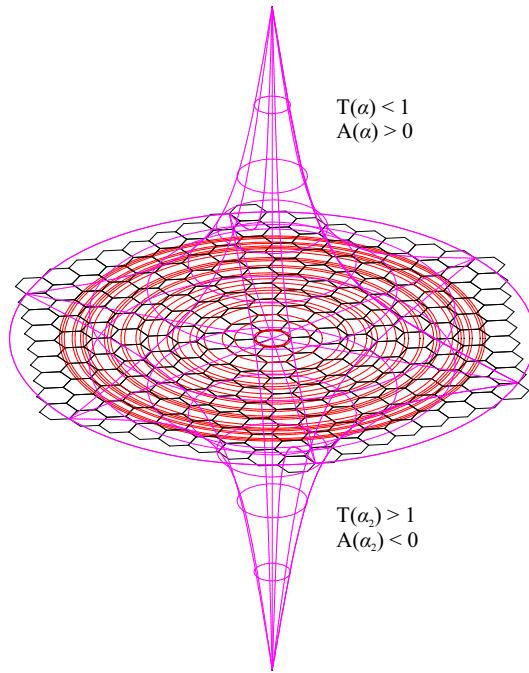
Figure A1. Illustration of the concepts of negative absorptance and excessive transmittance of EMR under normal incidence on MLG.

Perhaps the negative A and T exceeding 100% for α_2 (11) or (15) could be explained in terms of spontaneous graphene emission.

Appendix D MLG Fresnel Equation and Euclid's Formula

The Fresnel equation for the normal incidence of EMR at the boundary of two media with refractive indices n_1 and n_2

$$R + T = \frac{(n_1 - n_2)^2}{(n_1 + n_2)^2} + \frac{(2\sqrt{n_1 n_2})^2}{(n_1 + n_2)^2} = 1, \tag{A10}$$

has the same form as the Euclid's formula for generating Pythagorean triples $a = k^2 - l^2$, $b = 2kl$, $c = k^2 + l^2$

$$\frac{(k^2 - l^2)^2}{(k^2 + l^2)^2} + \frac{(2kl)^2}{(k^2 + l^2)^2} = 1, \tag{A11}$$

with $k^2 = n_1$ and $l^2 = n_2$.

Substituting MLG reflectance (4) and the sum of transmittance (3) and absorptance (5) into the Fresnel equation (A10) yields

$$\frac{(n_1 - n_2)^2}{(n_1 + n_2)^2} = \frac{\frac{1}{4}\pi^2\alpha^2}{\left(1 + \frac{\pi\alpha}{2}\right)^2}, \quad \frac{4n_1 n_2}{(n_1 + n_2)^2} = \frac{1 + \pi\alpha}{\left(1 + \frac{\pi\alpha}{2}\right)^2}, \tag{A12}$$

which resolves to n_1 independent on α and two forms of n_2

$$n_1 = 1,$$
$$n_2(\alpha_*) = \frac{1}{1 + \pi\alpha_*} = \left\{-\frac{\alpha_2}{\alpha}, -\frac{\alpha}{\alpha_2}\right\} \approx \{0.9776, 1.0229\}, \tag{A13}$$

where α_* indicates α or α_2, satisfying $1 + \pi\alpha = 1/(1 + \pi\alpha_2)$, which corresponds to the identity (13). The refractive index $n_2 \approx 1.0229$ is close to the refractive index of liquid helium $n \approx 1.025$ at 3 K. The

refractive index $n_2 \approx 0.9776$ is close to the refractive index of water $n = 0.99999974 = 1 - 2.6 \times 10^{-7}$ for X-ray radiation at a photon wavelength of 0.04 nm. We note that the refractive index is related to the phase velocity of light, which does not carry information and can be faster than the speed of light in vacuum c.

Refractive indices (A13) correspond to the phase velocities

$$
\begin{aligned}
V\left(-\frac{\alpha_2}{\alpha}\right) &= -c\frac{\alpha}{\alpha_2} = -c_2, \\
V\left(-\frac{\alpha}{\alpha_2}\right) &= -c\frac{\alpha_2}{\alpha} = -\frac{c^2}{c_2} \approx 2.9307 \times 10^{+8} \text{ [m/s]}
\end{aligned}
\tag{A14}
$$

assuming the refractive indices (A13) are absolute ($n = c/V$) and using the relation (26).

On the other hand, substituting MLG R, T+A into the Euclid formula (A11) yields

$$
\begin{aligned}
k &= \left\{ \sqrt{\pi\alpha + 1}, -\sqrt{\pi\alpha + 1}, \sqrt{\frac{1}{\pi\alpha + 1}}, -\sqrt{\frac{1}{\pi\alpha + 1}} \right\} \approx \\
&\approx \{\pm 1.0114, \pm 0.9887\}, \\
l &= \{1, 1, 1, 1\},
\end{aligned}
\tag{A15}
$$

generating four right triangles with edges

$$
\begin{aligned}
a(\alpha) &= \left\{ \pi\alpha, \pi\alpha, \frac{-\pi\alpha}{\pi\alpha + 1}, \frac{-\pi\alpha}{\pi\alpha + 1} \right\} \approx \\
&\approx \{0.0229x2, -0.0224x2\}, \\
b(\alpha) &= \left\{ 2\sqrt{\pi\alpha + 1}, -2\sqrt{\pi\alpha + 1}, \frac{2}{\sqrt{\pi\alpha + 1}}, \frac{-2}{\sqrt{\pi\alpha + 1}} \right\} \approx \\
&\approx \{\pm 2.0228, \pm 1.9775\}, \\
c(\alpha) &= \left\{ \pi\alpha + 2, \pi\alpha + 2, \frac{\pi\alpha + 2}{\pi\alpha + 1}, \frac{\pi\alpha + 2}{\pi\alpha + 1} \right\} \approx \\
&\approx \{2.0229x2, 1.9776x2\},
\end{aligned}
\tag{A16}
$$

and

$$
\begin{aligned}
a(\alpha_2) &\approx \{-0.0224x2, 0.0229x2\}, \\
b(\alpha_2) &\approx \{\pm 1.9775, \pm 2.0228\}, \\
c(\alpha_2) &\approx \{1.9776x2, 2.0229x2\},
\end{aligned}
\tag{A17}
$$

satisfying $\pi\alpha = -\pi\alpha_2/(\pi\alpha_2 + 1)$, which also corresponds to the identity (13), and

$$
c(\alpha_*) - a(\alpha_*) = 2, \quad b(\alpha_*)^2 = 4\sqrt{a(\alpha_*) + 1}.
\tag{A18}
$$

We further note that $a(\alpha_*) \approx -A(\alpha_*)$, (A6), (A8) and $|b(\alpha_*)| \approx T(\alpha_*) + 1$, (A5), (A7).

Appendix E Two π-Like Constants

The quadratic equation (8) that describes the reflectance R of MLG under the normal incidence of EMR can also be solved for π, which yields two roots.

$$
\pi(R, \alpha_*)_1 = \frac{2\sqrt{R}}{\alpha_*(1 - \sqrt{R})}, \quad \text{and}
\tag{A19}
$$

$$\pi(R, \alpha_*)_2 = \frac{-2\sqrt{R}}{\alpha_*(1 + \sqrt{R})}, \tag{A20}$$

dependent on R and α_*, where α_* indicates α or α_2. This can be further evaluated using the MLG reflectance R (4) or (A9) (which is the same for both α and α_2), yielding four, yet only three distinct possibilities

$$\pi_1 = \pi(\alpha)_1 = -\pi \frac{4\pi^2 + \pi + 1}{4\pi^2 + \pi + 2} = \pi \frac{\alpha_2}{\alpha} \approx -3.0712, \tag{A21}$$

$$\pi(\alpha)_2 = \pi(\alpha_2)_1 = \pi \approx 3.1416, \quad \text{and} \tag{A22}$$

$$\pi_2 = \pi(\alpha_2)_2 = -\pi \frac{4\pi^2 + \pi + 2}{4\pi^2 + \pi + 1} = \pi \frac{\alpha}{\alpha_2} \approx -3.2136. \tag{A23}$$

The modulus of π_1 (A21) corresponds to a convex surface having a positive Gaussian curvature, whereas the modulus of π_2 (A23) - to a negative Gaussian curvature. The product $\pi_1\pi_2 = \pi^2$ is independent of α_*, their quotient $\pi_1/\pi_2 = \alpha_2^2/\alpha^2$ is not directly dependent of π, and $|\pi_1 - \pi| \neq |\pi - \pi_2|$. It remains to be found whether each of these π-like constants describes the ratio of the circumference of a circle drawn on the respective surface to its diameter (π_c) or the ratio of the area of this circle to the square of its radius (π_a). These definitions produce different results on curved surfaces, whereas $\pi_a > \pi_c$ on convex surfaces, while $\pi_a < \pi_c$ on saddle surfaces [101].

Appendix F Why α-Space Is Better For Biological Evolution?

The probability of two nuclear *particles a* and *b* to undergo nuclear fusion by overcoming their electrostatic barriers is given by Gamow–Sommerfeld factor

$$p(E) = e^{-\sqrt{\frac{E_G}{E}}}, \tag{A24}$$

where

$$E_G := 2\frac{m_a m_b}{m_a + m_b} E_P (\pi \alpha Z_a Z_b)^2 \tag{A25}$$

is the Gamow energy, m_a, m_b are masses of those *particles* in terms of α- or α_2-Planck units (46) and Z_a, Z_b are their respective atomic numbers.

Since $(\pi\alpha)^2 \approx 5.2557 \times 10^{-4}$ is larger than $(\pi\alpha_2)^2 \approx 5.0227 \times 10^{-4}$, the probability (A24) is higher for the same dimensionless parameters m_*, Z_*. Therefore, perceivable α-space yields more favorable conditions for the evolution of information (by nuclear fusion) than nonperceivable α_2-space.

Furthermore, the α_2-Planck energy E_{Pi} and temperature T_{Pi} are higher than the Planck energy E_P and temperature T_P. Therefore, perceivable α-space yields more favorable conditions for the evolution of information, also due to the minimum energy principle.

Appendix G Planck Units and HUP

Perhaps the simplest derivation of the squared Planck length is based on HUP

$$\delta P_{\text{HUP}} \delta R_{\text{HUP}} \geq \frac{\hbar}{2} \quad \text{or} \quad \delta E_{\text{HUP}} \delta t_{\text{HUP}} \geq \frac{\hbar}{2}, \tag{A26}$$

where δP_{HUP}, δR_{HUP}, δE_{HUP}, and δt_{HUP} denote momentum, position, energy, and time uncertainties, by replacing energy uncertainty $\delta E_{\text{HUP}} = \delta M_{\text{HUP}} c^2$ with mass uncertainty using mass-energy equivalence, and time uncertainty with position uncertainty using $\delta t_{\text{HUP}} = \delta R_{\text{HUP}}/c$ [32], which yields

$$\delta M_{\text{HUP}} \delta R_{\text{HUP}} \geq \frac{\hbar}{2c}. \tag{A27}$$

Interpreting $\delta M_{\text{HUP}} = \delta R_{\text{HUP}} c^2/(2G)$ as the BH mass in (A27) we derive the Planck length as $\delta R_{\text{HUP}}^2 = \ell_P^2 \Rightarrow \delta D_{\text{HUP}} = \pm 2\ell_P$ and recover [5] the BH diameter $d_{\text{BH}} = \pm 2$.

However, using the same procedure but inserting the BH radius, instead of the BH mass, into the uncertainty principle (A27) leads to $\delta M_{\text{HUP}}^2 = \frac{1}{4}\hbar c/G = \frac{1}{4}m_{\text{P}}^2$. In general, using the generalized radius (49) in both procedures, one obtains

$$\delta M_{\text{HUP}}^2 = \frac{1}{2k}m_{\text{P}}^2 \quad \text{and} \quad \delta R_{\text{HUP}}^2 = \frac{k}{2}\ell_{\text{P}}^2. \tag{A28}$$

Thus, if k increases mass δM_{HUP} decreases, and δR_{HUP} increases and the factor is the same for $k = 1$ i.e., for *orbital speed radius* $\delta R = G\delta M/c^2$ or the *orbital speed mass* $\delta M = \delta Rc^2/G$.

Appendix H The Stoney Units Derivation

We assume that the elementary charge is the unit of charge $q_{\text{S}} = e$ and that the speed of light is the quotient of the unit of length and time $c = l_{\text{S}}/t_{\text{S}}$. Next, we compare the Coulomb force between two elementary charges and units of masses m_{S} with Newton's law of gravity, acting over the same distance

$$\frac{1}{4\pi\epsilon_0}\frac{e^2}{R^2} = G\frac{m_{\text{S}}^2}{R^2} \Rightarrow m_{\text{S}} = \pm\sqrt{\frac{e^2}{4\pi\epsilon_0 G}}. \tag{A29}$$

Finally, we compare the inertial force of the unit of mass with Newton's law of gravity

$$m_{\text{S}}\frac{\ell_{\text{S}}}{t_{\text{S}}^2} = G\frac{m_{\text{S}}^4}{\ell_{\text{S}}^2} \Rightarrow \ell_{\text{S}} = \pm\sqrt{\frac{Ge^2}{4\pi\epsilon_0 c^4}}, \tag{A30}$$

to derive the Stoney length ℓ_{S} and the remaining Stoney units.

Using the negative c_2 (22) we can determine the values of c_2-Stoney units (Sn). For mass, length, time, and energy they are

$$\begin{aligned}
m_{\text{S}n} &= m_{\text{S}} = \sqrt{\alpha}m_{\text{P}} \approx 0.0854m_{\text{P}}, \\
\ell_{\text{S}n} &= \frac{\alpha_2^2}{\alpha^2}\ell_{\text{S}} \approx 0.9557l_{\text{S}} \approx 0.0816l_{\text{P}}, \\
t_{\text{S}n} &= \frac{\alpha_2^3}{\alpha^3}t_{\text{S}} \approx -0.9343t_{\text{S}} \approx -0.0798t_{\text{P}}, \\
E_{\text{S}n} &= m_{\text{S}}c_2^2 = \frac{\alpha^2}{\alpha_2^2}E_{\text{S}} \approx 1.0464E_{\text{S}} \approx 0.0894E_{\text{P}}.
\end{aligned} \tag{A31}$$

We note that the c_2-Stoney energy induced by c_2 is greater than the Stoney energy and the c_2-Stoney time *runs* in the opposite direction. We also note that the negative value of the gravitational constant G would yield imaginary Stoney units regardless of the sign of c, as all Stoney units (except charge) contain c raised to even (4, 6) powers.

Appendix I Hall Effect

The fractional quantum Hall (FQHE) effect shows a stepwise dependence of the conductance on the magnetic field (as compared to a linear dependence of the Hall effect) with steps quantized as

$$R = \frac{h}{ve^2} = \frac{2\pi\hbar}{v\alpha 4\pi\epsilon_0\hbar c} = \frac{1}{2v\epsilon_0\alpha c} = \frac{1}{2v\epsilon_0\alpha_2 c_2}, \tag{A32}$$

where v is an integer or fraction (for example, for $v = 5/2$, $R = 1/(5\epsilon_0\alpha c)$). Relations (A32) and (26) suggest that 2D FQHE links real and imaginary dimensions similarly to 2D graphene, giving us the second negative fine-structure constant α_2.

References

1.   P. T. de Chardin, *The Phenomenon of Man*. Harper, New York, 1959.
2.   I. Prigogine and I. Stengers, *Order out of Chaos: Man's New Dialogue with Nature*. Bantam Books, 1984.
3.   R. Melamede, "Dissipative structures and the origins of life," in *Unifying Themes in Complex Systems IV* (A. A. Minai and Y. Bar-Yam, eds.), (Berlin, Heidelberg), pp. 80–87, Springer Berlin Heidelberg, 2008.
4.   V. Vedral, *Decoding Reality: The Universe as Quantum Information*. Oxford University Press, 2010.
5.   S. Łukaszyk, *Black Hole Horizons as Patternless Binary Messages and Markers of Dimensionality*, ch. 15, pp. 317–374. Nova Science Publishers, 2023.
6.   M. M. Vopson and S. Lepadatu, "Second law of information dynamics," *AIP Advances*, vol. 12, p. 075310, July 2022.
7.   "Platonic Solids in All Dimensions."
8.   C. H. Taubes, "Gauge theory on asymptotically periodic {4}-manifolds," *Journal of Differential Geometry*, vol. 25, Jan. 1987.
9.   S. Łukaszyk, "Four Cubes," Feb. 2021. arXiv:2007.03782 [math].
10. S. Lukaszyk, "Solving the black hole information paradox," *Research Outreach*, Feb. 2023.
11. Č. Brukner, "A No-Go Theorem for Observer-Independent Facts," *Entropy*, vol. 20, no. 5, 2018.
12. S. Łukaszyk, "Life as the Explanation of the Measurement Problem," 2018.
13. S. Łukaszyk, "Novel Recurrence Relations for Volumes and Surfaces of n-Balls, Regular n-Simplices, and n-Orthoplices in Real Dimensions," *Mathematics*, vol. 10, p. 2212, June 2022.
14. S. Łukaszyk and A. Tomski, "Omnidimensional Convex Polytopes," *Symmetry*, vol. 15, Mar. 2023.
15. M. Planck, "Über irreversible Strahlungsvorgänge," 1899.
16. G. J. Stoney, "LII. *On the physical units of nature*," *The London, Edinburgh, and Dublin Philosophical Magazine and Journal of Science*, vol. 11, pp. 381–390, May 1881.
17. X. Peng, H. Zhou, B.-B. Wei, J. Cui, J. Du, and R.-B. Liu, "Experimental Observation of Lee-Yang Zeros," *Physical Review Letters*, vol. 114, p. 010601, Jan. 2015.
18. K. Gnatenko, A. Kargol, and V. Tkachuk, "Lee–Yang zeros and two-time spin correlation function," *Physica A: Statistical Mechanics and its Applications*, vol. 509, pp. 1095–1101, Nov. 2018.
19. A. L. Marques Muniz, F. O. Wu, P. S. Jung, M. Khajavikhan, D. N. Christodoulides, and U. Peschel, "Observation of photon-photon thermodynamic processes under negative optical temperature conditions," *Science*, vol. 379, pp. 1019–1023, Mar. 2023.
20. S. Wang, Z. Hu, Q. Wu, H. Chen, E. Prodan, R. Zhu, and G. Huang, "Smart patterning for topological pumping of elastic surface waves," *Science Advances*, vol. 9, p. eadh4310, July 2023.
21. M. Wurdack, T. Yun, M. Katzer, A. G. Truscott, A. Knorr, M. Selig, E. A. Ostrovskaya, and E. Estrecho, "Negative-mass exciton polaritons induced by dissipative light-matter coupling in an atomically thin semiconductor," *Nature Communications*, vol. 14, p. 1026, Feb. 2023.
22. A. B. Kuzmenko, E. van Heumen, F. Carbone, and D. van der Marel, "Universal dynamical conductance in graphite," *Physical Review Letters*, vol. 100, p. 117401, Mar. 2008. arXiv:0712.0835 [cond-mat].
23. K. F. Mak, M. Y. Sfeir, Y. Wu, C. H. Lui, J. A. Misewich, and T. F. Heinz, "Measurement of the Optical Conductivity of Graphene," *Physical Review Letters*, vol. 101, p. 196405, Nov. 2008.
24. R. R. Nair, P. Blake, A. N. Grigorenko, K. S. Novoselov, T. J. Booth, T. Stauber, N. M. R. Peres, and A. K. Geim, "Universal Dynamic Conductivity and Quantized Visible Opacity of Suspended Graphene," *Science*, vol. 320, pp. 1308–1308, June 2008. arXiv:0803.3718 [cond-mat].
25. T. Stauber, N. M. R. Peres, and A. K. Geim, "Optical conductivity of graphene in the visible region of the spectrum," *Physical Review B*, vol. 78, p. 085432, Aug. 2008.
26. X. Wang and B. Chen, "Origin of Fresnel problem of two dimensional materials," *Scientific Reports*, vol. 9, p. 17825, Dec. 2019.
27. M. Merano, "Fresnel coefficients of a two-dimensional atomic crystal," *Physical Review A*, vol. 93, p. 013832, Jan. 2016.
28. T. Ando, Y. Zheng, and H. Suzuura, "Dynamical Conductivity and Zero-Mode Anomaly in Honeycomb Lattices," *Journal of the Physical Society of Japan*, vol. 71, pp. 1318–1324, May 2002.
29. S.-E. Zhu, S. Yuan, and G. C. A. M. Janssen, "Optical transmittance of multilayer graphene," *EPL (Europhysics Letters)*, vol. 108, p. 17007, Oct. 2014.

30. I. G. Ivanov, J. U. Hassan, T. Iakimov, A. A. Zakharov, R. Yakimova, and E. Janzén, "Layer-number determination in graphene on SiC by reflectance mapping," *Carbon*, vol. 77, pp. 492–500, Oct. 2014.

31. P. Varlaki, L. Nadai, and J. Bokor, "Number Archetypes in System Realization Theory Concerning the Fine Structure Constant," in *2008 International Conference on Intelligent Engineering Systems*, (Miami, FL), pp. 83–92, IEEE, Feb. 2008.

32. F. Scardigli, "Some heuristic semi-classical derivations of the Planck length, the Hawking effect and the Unruh effect," *Il Nuovo Cimento B (1971-1996)*, vol. 110, no. 9, pp. 1029–1034, 1995.

33. M. E. Tobar, "Global representation of the fine structure constant and its variation," *Metrologia*, vol. 42, pp. 129–133, Apr. 2005.

34. E. G. Haug, "Finding the Planck length multiplied by the speed of light without any knowledge of *G*, *c*, or *h*, using a Newton force spring," *Journal of Physics Communications*, vol. 4, p. 075001, July 2020.

35. E. K. Anderson, C. J. Baker, W. Bertsche, N. M. Bhatt, G. Bonomi, A. Capra, I. Carli, C. L. Cesar, M. Charlton, A. Christensen, R. Collister, A. Cridland Mathad, D. Duque Quiceno, S. Eriksson, A. Evans, N. Evetts, S. Fabbri, J. Fajans, A. Ferwerda, T. Friesen, M. C. Fujiwara, D. R. Gill, L. M. Golino, M. B. Gomes Gonçalves, P. Grandemange, P. Granum, J. S. Hangst, M. E. Hayden, D. Hodgkinson, E. D. Hunter, C. A. Isaac, A. J. U. Jimenez, M. A. Johnson, J. M. Jones, S. A. Jones, S. Jonsell, A. Khramov, N. Madsen, L. Martin, N. Massacret, D. Maxwell, J. T. K. McKenna, S. Menary, T. Momose, M. Mostamand, P. S. Mullan, J. Nauta, K. Olchanski, A. N. Oliveira, J. Peszka, A. Powell, C. Rasmussen, F. Robicheaux, R. L. Sacramento, M. Sameed, E. Sarid, J. Schoonwater, D. M. Silveira, J. Singh, G. Smith, C. So, S. Stracka, G. Stutter, T. D. Tharp, K. A. Thompson, R. I. Thompson, E. Thorpe-Woods, C. Torkzaban, M. Urioni, P. Woosaree, and J. S. Wurtele, "Observation of the effect of gravity on the motion of antimatter," *Nature*, vol. 621, pp. 716–722, Sept. 2023.

36. X. Lin, R. Du, and X. Xie, "Recent experimental progress of fractional quantum Hall effect: 5/2 filling state and graphene," *National Science Review*, vol. 1, pp. 564–579, Dec. 2014.

37. E. Verlinde, "On the origin of gravity and the laws of Newton," *Journal of High Energy Physics*, vol. 2011, p. 29, Apr. 2011.

38. L. Schneider, K. T. Ton, I. Ioannidis, J. Neuhaus-Steinmetz, T. Posske, R. Wiesendanger, and J. Wiebe, "Proximity superconductivity in atom-by-atom crafted quantum dots," *Nature*, Aug. 2023.

39. R. Hiller, S. J. Putterman, and B. P. Barber, "Spectrum of synchronous picosecond sonoluminescence," *Physical Review Letters*, vol. 69, pp. 1182–1184, Aug. 1992.

40. C. Eberlein, "Theory of quantum radiation observed as sonoluminescence," *Physical Review A*, vol. 53, pp. 2772–2787, Apr. 1996.

41. D. Lohse, B. Schmitz, and M. Versluis, "Snapping shrimp make flashing bubbles," *Nature*, vol. 413, pp. 477–478, Oct. 2001.

42. E. A. Rietman, B. Melcher, A. Bobrick, and G. Martire, "A Cylindrical Optical-Space Black Hole Induced from High-Pressure Acoustics in a Dense Fluid," *Universe*, vol. 9, p. 162, Mar. 2023.

43. F. Melia, "A Candid Assessment of Standard Cosmology," *Publications of the Astronomical Society of the Pacific*, vol. 134, p. 121001, Dec. 2022.

44. M. Boylan-Kolchin, "Stress testing λCDM with high-redshift galaxy candidates," *Nature Astronomy*, Apr. 2023.

45. S. Lukaszyk, "A No-go Theorem for Superposed Actions (Making Schrödinger's Cat Quantum Nonlocal)," in *New Frontiers in Physical Science Research Vol. 3* (D. J. Purenovic, ed.), pp. 137–151, Book Publisher International (a part of SCIENCEDOMAIN International), Nov. 2022. arXiv:1801.08537 [quant-ph].

46. K. Qian, K. Wang, L. Chen, Z. Hou, M. Krenn, S. Zhu, and X.-s. Ma, "Multiphoton non-local quantum interference controlled by an undetected photon," *Nature Communications*, vol. 14, p. 1480, Mar. 2023.

47. P. Xue, L. Xiao, G. Ruffolo, A. Mazzari, T. Temistocles, M. T. Cunha, and R. Rabelo, "Synchronous Observation of Bell Nonlocality and State-Dependent Contextuality," *Physical Review Letters*, vol. 130, p. 040201, Jan. 2023.

48. D. M. Tran, V.-D. Nguyen, L. B. Ho, and H. Q. Nguyen, "Increased success probability in hardy's nonlocality: Theory and demonstration," *Phys. Rev. A*, vol. 107, p. 042210, Apr 2023.

49. P. Colciaghi, Y. Li, P. Treutlein, and T. Zibold, "Einstein-podolsky-rosen experiment with two bose-einstein condensates," *Phys. Rev. X*, vol. 13, p. 021031, May 2023.

50. S. Watanabe, *Knowing and Guessing: A Quantitative Study of Inference and Information*. Wiley, January 1969.

51. S. Watanabe, "Epistemological Relativity," *Annals of the Japan Association for Philosophy of Science*, vol. 7, no. 1, pp. 1–14, 1986.

52. I. Saeed, H. K. Pak, and T. Tlusty, "Quasiparticles, flat bands and the melting of hydrodynamic matter," *Nature Physics*, Jan. 2023.

53. S. Comerón, I. Trujillo, M. Cappellari, F. Buitrago, L. E. Garduño, J. Zaragoza-Cardiel, I. A. Zinchenko, M. A. Lara-López, A. Ferré-Mateu, and S. Dib, "The massive relic galaxy NGC 1277 is dark matter deficient: From dynamical models of integral-field stellar kinematics out to five effective radii," *Astronomy & Astrophysics*, vol. 675, p. A143, July 2023.

54. M. M. Brouwer *et al.*, "First test of verlinde's theory of emergent gravity using weak gravitational lensing measurements," *Monthly Notices of the Royal Astronomical Society*, vol. 466, pp. 2547–2559, April 2017.

55. A. J. Schimmoller, G. McCaul, H. Abele, and D. I. Bondar, "Decoherence-free entropic gravity: Model and experimental tests," *Physical Review Research*, vol. 3, p. 033065, July 2021.

56. F. M. Vincentelli and et al., "A shared accretion instability for black holes and neutron stars," *Nature*, vol. 615, pp. 45–49, Mar. 2023.

57. V. Valenzuela-Villaseca, L. Suttle, F. Suzuki-Vidal, J. Halliday, S. Merlini, D. Russell, E. Tubman, J. Hare, J. Chittenden, M. Koepke, E. Blackman, and S. Lebedev, "Characterization of Quasi-Keplerian, Differentially Rotating, Free-Boundary Laboratory Plasmas," *Physical Review Letters*, vol. 130, p. 195101, May 2023.

58. G. J. Chaitin, "On the Length of Programs for Computing Finite Binary Sequences," *J. ACM*, vol. 13, p. 547–569, oct 1966.

59. S. Hawking, "Black hole explosions?," *Nature*, vol. 248, pp. 30–31, 1974.

60. P. M. Alsing and G. J. Milburn, "Teleportation with a Uniformly Accelerated Partner," *Phys. Rev. Lett.*, vol. 91, p. 180404, Oct 2003.

61. J. D. Bekenstein, "Black Holes and Entropy," *Phys. Rev. D*, vol. 7, pp. 2333–2346, Apr 1973.

62. G. t. Hooft, "Dimensional Reduction in Quantum Gravity," 1993.

63. A. Gould, "Classical derivation of black-hole entropy," *Physical Review D*, vol. 35, pp. 449–454, Jan. 1987.

64. R. Penrose and R. M. Floyd, "Extraction of Rotational Energy from a Black Hole," *Nature Physical Science*, vol. 229, pp. 177–179, Feb. 1971.

65. D. Christodoulou and R. Ruffini, "Reversible Transformations of a Charged Black Hole," *Physical Review D*, vol. 4, pp. 3552–3555, Dec. 1971.

66. Z. Stuchlík, M. Kološ, and A. Tursunov, "Penrose Process: Its Variants and Astrophysical Applications," *Universe*, vol. 7, p. 416, Oct. 2021.

67. A. Sneppen, D. Watson, A. Bauswein, O. Just, R. Kotak, E. Nakar, D. Poznanski, and S. Sim, "Spherical symmetry in the kilonova AT2017gfo/GW170817," *Nature*, vol. 614, pp. 436–439, Feb. 2023.

68. T. Zhang, "Electric Charge as a Form of Imaginary Energy," Apr. 2008.

69. B. Schrinski, Y. Yang, U. Von Lüpke, M. Bild, Y. Chu, K. Hornberger, S. Nimmrichter, and M. Fadel, "Macroscopic Quantum Test with Bulk Acoustic Wave Resonators," *Physical Review Letters*, vol. 130, p. 133604, Mar. 2023.

70. B. R. Iyer, C. V. Vishveshwara, and S. V. Dhurandhar, "Ultracompact (R<3 M) objects in general relativity," *Classical and Quantum Gravity*, vol. 2, pp. 219–228, Mar. 1985.

71. R. J. Nemiroff, P. A. Becker, and K. S. Wood, "Properties of ultracompact neutron stars," *The Astrophysical Journal*, vol. 406, p. 590, Apr. 1993.

72. A. P. Lightman, W. H. Press, R. H. Price, and S. A. Teukolsky, *Problem Book in Relativity and Gravitation*. Princeton University Press, Sept. 2017.

73. S. Weinberg, *Gravitation and cosmology: Principles and applications of the general theory of relativity*. New York: Wiley, 1972.

74. M. S. Morris and K. S. Thorne, "Wormholes in spacetime and their use for interstellar travel: A tool for teaching general relativity," *American Journal of Physics*, vol. 56, pp. 395–412, May 1988.

75. K. R. Pechenick, C. Ftaclas, and J. M. Cohen, "Hot spots on neutron stars - The near-field gravitational lens," *The Astrophysical Journal*, vol. 274, p. 846, Nov. 1983.

76. C. Montgomery, W. Orchiston, and I. Whittingham, "Michell, Laplace and the Origin of the Black Hole Concept," *Journal of Astronomical History and Heritage*, vol. 12, pp. 90–96, July 2009.

77. K. Szostek and R. Szostek, "The derivation of the general form of kinematics with the universal reference system," *Results in Physics*, vol. 8, pp. 429–437, Mar. 2018.

78. R. Szostek, "The Original Method of Deriving Transformations for Kinematics with a Universal Reference System," *Jurnal Fizik Malaysia*, vol. 43, pp. 10244–10263, 2022.

79. R. Szostek and K. Szostek, "The Existence of a Universal Frame of Reference, in Which it Propagates Light, is Still an Unresolved Problem of Physics," *Jordan Journal of Physics*, vol. 15, pp. 457–467, Dec. 2022.

80. R. Szostek, "Explanation of What Time in Kinematics Is and Dispelling Myths Allegedly Stemming from the Special Theory of Relativity," *Applied Sciences*, vol. 12, p. 6272, June 2022.

81. C. S. Unnikrishnan, "Cosmic Gravity and the Quantum Spin," in *New Relativity in the Gravitational Universe*, vol. 209, pp. 373–405, Cham: Springer International Publishing, 2022.

82. C. S. Unnikrishnan, "Cosmic Relativity—The Theory and Its Primary Fundamental Results," in *New Relativity in the Gravitational Universe*, vol. 209, pp. 255–306, Cham: Springer International Publishing, 2022.

83. Szostek, Karol and Szostek, Roman, "The concept of a mechanical system for measuring the one-way speed of light," *Technical Transactions*, vol. 2023, no. 1, pp. 1–9, 2023.

84. B. P. Abbott and et al., "GW170817: Observation of Gravitational Waves from a Binary Neutron Star Inspiral," *Physical Review Letters*, vol. 119, p. 161101, Oct. 2017.

85. R. Szostek, P. Góralski, and K. Szostek, "Gravitational waves in Newton's gravitation and criticism of gravitational waves resulting from the General Theory of Relativity (LIGO)," *Bulletin of the Karaganda University. "Physics" Series*, vol. 96, pp. 39–56, Dec. 2019.

86. D. Li, P. Wagle, Y. Chen, and N. Yunes, "Perturbations of Spinning Black Holes beyond General Relativity: Modified Teukolsky Equation," *Physical Review X*, vol. 13, p. 021029, May 2023.

87. S. W. Hawking, ed., *Three hundred years of gravitation*. Cambridge: Cambridge University Press, transferred to digital print ed., 2003.

88. V. Kalogera and G. Baym, "The Maximum Mass of a Neutron Star," *The Astrophysical Journal*, vol. 470, pp. L61–L64, Oct. 1996.

89. S. Ai, H. Gao, and B. Zhang, "What Constraints on the Neutron Star Maximum Mass Can One Pose from GW170817 Observations?," *The Astrophysical Journal*, vol. 893, p. 146, Apr. 2020.

90. A. Moroianu, L. Wen, C. W. James, S. Ai, M. Kovalam, F. H. Panther, and B. Zhang, "An assessment of the association between a fast radio burst and binary neutron star merger," *Nature Astronomy*, Mar. 2023.

91. D. Lai, "IXPE detection of polarized X-rays from magnetars and photon mode conversion at QED vacuum resonance," *Proceedings of the National Academy of Sciences*, vol. 120, p. e2216534120, Apr. 2023.

92. R. Anna-Thomas, L. Connor, S. Dai, Y. Feng, S. Burke-Spolaor, P. Beniamini, Y.-P. Yang, Y.-K. Zhang, K. Aggarwal, C. J. Law, D. Li, C. Niu, S. Chatterjee, M. Cruces, R. Duan, M. D. Filipovic, G. Hobbs, R. S. Lynch, C. Miao, J. Niu, S. K. Ocker, C.-W. Tsai, P. Wang, M. Xue, J.-M. Yao, W. Yu, B. Zhang, L. Zhang, S. Zhu, and W. Zhu, "Magnetic field reversal in the turbulent environment around a repeating fast radio burst," *Science*, vol. 380, pp. 599–603, May 2023.

93. L. Susskind, *Black Hole War: My Battle with Stephen Hawking to Make the World Safe for Quantum Mechanics*. Little, Brown and Company, 2008.

94. H. Jussila, H. Yang, N. Granqvist, and Z. Sun, "Surface plasmon resonance for characterization of large-area atomic-layer graphene film," *Optica*, vol. 3, p. 151, Feb. 2016.

95. P. R. Wallace, "Erratum: The Band Theory of Graphite [Phys. Rev. 71, 622 (1947)]," *Physical Review*, vol. 72, pp. 258–258, Aug. 1947.

96. K. S. Novoselov, A. K. Geim, S. V. Morozov, D. Jiang, Y. Zhang, S. V. Dubonos, I. V. Grigorieva, and A. A. Firsov, "Electric Field Effect in Atomically Thin Carbon Films," *Science*, vol. 306, pp. 666–669, Oct. 2004.

97. A. Einstein, B. Podolsky, and N. Rosen, "Can Quantum-Mechanical Description of Physical Reality Be Considered Complete?," *Physical Review*, vol. 47, pp. 777–780, May 1935.

98. J. S. Bell, "On the Einstein Podolsky Rosen paradox," *Physics Physique Fizika*, vol. 1, pp. 195–200, Nov. 1964.

99. S. Łukaszyk, "A short note about graphene and the fine structure constant," 2020.

100. S. Łukaszyk, "A short note about the geometry of graphene," 2020.

101. S. Mahajan, "Calculation of the pi-like circular constants in curved geometry." ResearchGate, Nov. 2013.